

NO-A166 560

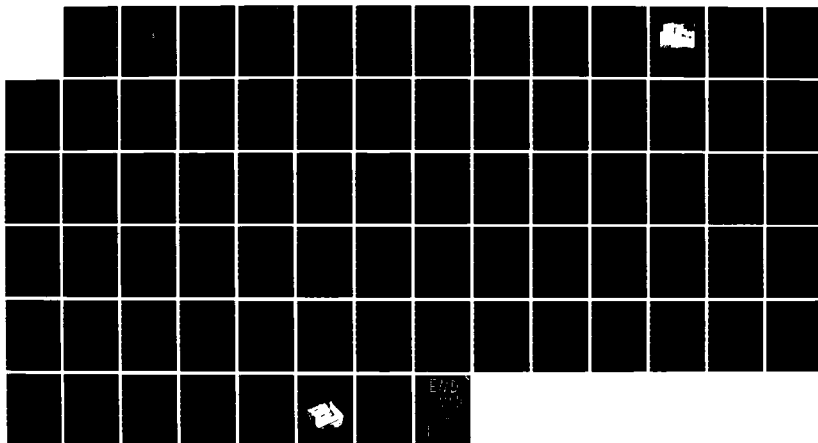
POSITIVE ION EJECTION SYSTEM (PIES)(U) HUGHES RESEARCH
LABS MALIBU CA R ROBSON ET AL. SEP 85 AFGL-TR-85-0251
F19628-83-C-0057

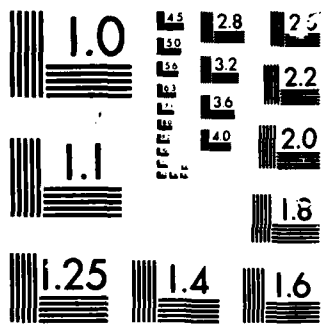
1/1

UNCLASSIFIED

F/G 20/3

NL





MICROCOPY

CHART

12

AFGL-TR-85-0251

POSITIVE ION EJECTION SYSTEM (PIES)

AD-A166 560

R. Robson, W. Williamson, and J. Hyman

Hughes Research Laboratories
3011 Malibu Canyon Road
Malibu, CA 90265

DTIC
S
APR 15 1986
D

September 1985

Final Report

14 March 1983 through 30 April 1985

Approved for public release; distribution unlimited

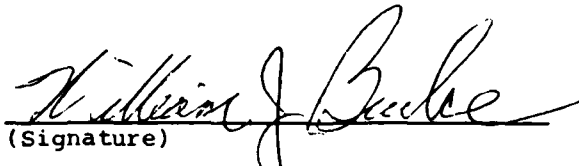
AIR FORCE GEOPHYSICS LABORATORY
AIR FORCE SYSTEMS COMMAND
UNITED STATES AIR FORCE
HANSCOM AIR FORCE BASE, MASSACHUSETTS 01731

ATP FILE COPY

107

"This technical report has been reviewed and is approved for publication"

FOR THE COMMANDER


(Signature)
WILLIAM J. BURKE
Branch Chief


(Signature)
RITA C. SAGALYN
Division Director

This document has been reviewed by the ESD Public Affairs Office (PA) and is releasable to the National Technical Information Service (NTIS)

Qualified requestors may obtain additional copies from the Defense Technical Information Center. All others should apply to the National Technical Information Service.

If your address has changed, or if you wish to be removed from the mailing list, or if the addressee is no longer employed by your organization, please notify AFGL/DAA, Hanscom AFB, MA 01731. This will assist us in maintaining a current mailing list.

UNCLASSIFIED

SECURITY CLASSIFICATION OF THIS PAGE

AD-A166560

REPORT DOCUMENTATION PAGE

1a. REPORT SECURITY CLASSIFICATION UNCLASSIFIED		1b. RESTRICTIVE MARKINGS										
2a. SECURITY CLASSIFICATION AUTHORITY		3. DISTRIBUTION/AVAILABILITY OF REPORT Approved for public release; distribution unlimited.										
2b. DECLASSIFICATION/DOWNGRADING SCHEDULE												
4. PERFORMING ORGANIZATION REPORT NUMBER(S) .		5. MONITORING ORGANIZATION REPORT NUMBER(S) AFGL-TR-85-0251										
6a. NAME OF PERFORMING ORGANIZATION Hughes Research Laboratories	6b. OFFICE SYMBOL (If applicable)	7a. NAME OF MONITORING ORGANIZATION Air Force Geophysics Laboratory										
6c. ADDRESS (City, State and ZIP Code) 3011 Malibu Canyon Road Malibu, CA 90265		7b. ADDRESS (City, State and ZIP Code) Hanscom AFB, MA 01731										
8a. NAME OF FUNDING/SPONSORING ORGANIZATION Electronics Systems Div., AFGL	8b. OFFICE SYMBOL (If applicable) AFGL/PHG	9. PROCUREMENT INSTRUMENT IDENTIFICATION NUMBER F19628-83-C-0057										
8c. ADDRESS (City, State and ZIP Code) Hanscom AFB, MA 01731		10. SOURCE OF FUNDING NOS. <table border="1"><tr><td>PROGRAM ELEMENT NO.</td><td>PROJECT NO.</td><td>TASK NO.</td><td>WORK UNIT NO.</td></tr><tr><td>62101F</td><td>7661</td><td>14</td><td>AC</td></tr></table>		PROGRAM ELEMENT NO.	PROJECT NO.	TASK NO.	WORK UNIT NO.	62101F	7661	14	AC	
PROGRAM ELEMENT NO.	PROJECT NO.	TASK NO.	WORK UNIT NO.									
62101F	7661	14	AC									
11. TITLE (Include Security Classification) Positive Ion Ejection System (PIES)												
12. PERSONAL AUTHOR(S) R. Robson, W. Williamson, and J. Hyman												
13a. TYPE OF REPORT Final Report	13b. TIME COVERED FROM 3-14-83 TO 4-30-85	14. DATE OF REPORT (Yr., Mo., Day) September 1985	15. PAGE COUNT 82									
16. SUPPLEMENTARY NOTATION												
17. COSATI CODES <table border="1"><tr><td>FIELD</td><td>GROUP</td><td>SUB GR.</td></tr><tr><td></td><td></td><td></td></tr><tr><td></td><td></td><td></td></tr></table>		FIELD	GROUP	SUB GR.							18. SUBJECT TERMS (Continue on reverse if necessary and identify by block number) Spacecraft Charging, Rocket Charging, PIES, Positive Ion Ejection System, Ion Beam, BERT I rocket	
FIELD	GROUP	SUB GR.										
19. ABSTRACT (Continue on reverse if necessary and identify by block number) Hughes Research Laboratories has designed, fabricated, tested, and delivered both a breadboard- and a flight-model Positive Ion Ejection System (PIES) to the Air Force Geophysics Laboratory. The flight-model system will be employed to eject positive charge from a rocket (BERT I) in order to simulate and investigate spacecraft charging. The PIES models each consist of an argon-ion source; an argon expellant tank; power, command, and telemetry electronics; and suitable packaging. The ion source emits an unneutralized argon-ion beam at selected voltages in the energy range from 0.5 to 4.5 keV, with selected ion-beam currents in the range of 0.02 to 20 mA. The flight-model PIES exhibits environmental-tolerance attributes suitable for rocket launch. Design considerations, final design configuration, and test data are presented.												
20. DISTRIBUTION/AVAILABILITY OF ABSTRACT UNCLASSIFIED/UNLIMITED <input checked="" type="checkbox"/> SAME AS RPT <input type="checkbox"/> DTIC USERS <input type="checkbox"/>		21. ABSTRACT SECURITY CLASSIFICATION UNCLASSIFIED										
22a. NAME OF RESPONSIBLE INDIVIDUAL H. Cohen		22b. TELEPHONE NUMBER (Include Area Code) (617) 861-3107	22c. OFFICE SYMBOL AFGL/PHG									

TABLE OF CONTENTS

SECTION		PAGE
1	INTRODUCTION.....	9
2	PIES SYSTEM.....	11
3	ION SOURCE.....	15
	3.1 Mechanical Design.....	15
	3.2 Filament Tests.....	19
	3.3 Charge Exchange.....	21
4	POWER ELECTRONICS UNIT (PEU).....	27
	4.1 Flyback Inverters.....	27
	4.2 Filament Supply.....	29
	4.3 Discharge Supply.....	31
	4.4 Accel Supply.....	31
	4.5 Screen Supply.....	35
	4.6 Housekeeping Inverter.....	35
	4.7 Log Electrometer.....	38
	4.8 Command and Telemetry Interface.....	38
5	EXPELLANT FEED SYSTEM.....	45
6	SYSTEM TESTING.....	51
7	GROUND SUPPORT EQUIPMENT (GSE).....	79

Accession For	
NTIS CRA&I	<input checked="" type="checkbox"/>
DTIC TAB	<input type="checkbox"/>
Unannounced	<input type="checkbox"/>
Justification	
By	
Distribution /	
Availability Codes	
Dist	Avail and/or Special
A-1	



LIST OF ILLUSTRATIONS

FIGURE		PAGE
2-1	Flight-model PIES mounted on a test fixture.....	12
3-1	PIES ion source assembly.....	16
3-2	Ion optics assembly.....	17
3-3	Details of each beam forming aperture.....	18
3-4	Original and simplified filament designs on their mounting brackets.....	22
4-1	Simplified schematic of a half-wave flyback inverter.....	28
4-2	Filament supply schematic.....	30
4-3	Discharge supply schematic.....	32
4-4	Output voltage-current characteristic of the discharge supply.....	33
4-5	Accel supply schematic.....	34
4-6	Screen supply schematic.....	36
4-7	Housekeeping inverter schematic.....	37
4-8	Analog control circuitry schematic.....	39
4-9	Calibration curve for the flight log electrometer.....	40
4-10	Digital control circuitry schematic.....	42
5-1	Expellant feed system configuration.....	46
5-2	Flowrate versus gas pressure for the porous-tungsten flow impedance.....	48
5-3	Time required to fill the ullage volume between the porous-tungsten plug and valve.....	49
6-1	Strip chart recording of beam energy and emission current during a sweep of the breadboard PIES.....	52

FIGURE		PAGE
6-2	System configuration for the breadboard and early testing of the flight hardware.....	54
6-3	Final system configuration of the PIES flight hardware.....	56
6-4	Emission-current feedback loop of the breadboard and during early testing of the flight hardware.....	57
6-5	Bode plots of the emission-current feedback loop for the breadboard and early testing of the flight hardware.....	58
6-6	Final emission-current feedback loop.....	59
6-7	Bode plots for the final emission-current feedback loop.....	60
6-8(a)	Response of the flight system as it steps through its current setpoints at a beam energy of 500 V.....	61
6-8(b)	Response of the flight system as it steps through its 16 current setpoints at a beam energy of 2 kV.....	62
6-8(c)	Response of the flight system as it steps through its 16 current setpoints at a beam energy of 4.5 kV.....	63
6-9	Input power required by the flight system for all operating points.....	68
6-10	Telemetry calibration curve for the discharge voltage.....	69
6-11	Telemetry calibration curve for the discharge current.....	69
6-12	Telemetry calibration curve for the filament voltage.....	70
6-13	Telemetry calibration curve for the filament current.....	70

FIGURE		PAGE
6-14	Telemetry calibration curve for the accel voltage.....	71
6-15	Telemetry calibration curve for the accel current.....	72
6-16	Telemetry calibration curve for the screen voltage.....	72
6-17	Telemetry calibration curve for the screen current.....	73
6-18	Telemetry calibration curve for the decel current.....	74
6-19	Telemetry calibration curve for the +5-V housekeeping supply.....	75
6-20	Telemetry calibration curve for the +15-V housekeeping supply.....	76
6-21	Telemetry calibration curve for the ullage volume pressure.....	77
7-1	Photograph of the ground support equipment.....	80
7-2	A typical printout from the GSE.....	81

SECTION 1

INTRODUCTION

Under this program, Hughes Research Laboratories (HRL) has designed, fabricated, tested, and delivered both a breadboard- and a flight-model Positive Ion Ejection System (PIES) to the Air Force Geophysics Laboratory. The flight-model system will be employed to eject positive charge from a rocket (BERT I) in order to simulate and investigate spacecraft charging. The PIES systems each consist of an argon-ion source; argon expellant tank; power, command, and telemetry electronics; and suitable packaging. The ion source emits an unneutralized argon-ion beam at selected voltages in the energy range from 0.5 to 4.5 keV with selected ion-beam currents in the range of 0.02 to 20 mA. The flight-model PIES exhibits environmental-tolerance attributes suitable for rocket launch.

SECTION 2

PIES SYSTEM

In Figure 2-1 the flight-model PIES is shown mounted to a test fixture, but is otherwise in the flight configuration. The electronics box will be mounted on a shelf inside a pressurized vessel (provided by the USAF) that is part of the rocket-payload body. The pressurized vessel simplifies the packaging of the electronics, since the thermal and high-voltage-breakdown problems associated with vacuum operation are not encountered. The expellant tank and feed system are mounted to another shelf and the ion source is mounted to the flat side of the pressure vessel. A blow-off cover will protect the ion source during the launch phase of the rocket flight.

The flight-model PIES is designed to meet the specifications listed in Table 2-1. The system was functionally tested by Hughes and environmentally tested (vibration, shock, and thermal-vacuum) by the USAF to show compliance with these specifications.

The flight hardware occupies a cylindrical volume in the rocket that is 43.2 cm (17 in.) in diameter and 26.7 cm (10.5 in.) high. The electronics box is 21 cm x 27.2 cm x 13 cm and the source is 17.2 cm in diameter, with an overall length of 16 cm.

The flight hardware (as delivered) weights 10.67 kg (23.5 lb), which is 0.68 kg (1.5 lb) less than the value that had earlier been estimated and 2.95 kg (6.5 lb) less than the maximum allowed by the contract. The electronics weight 4.97 kg (11.0 lb), the feed system weighs 2.27 kg (5.0 lb), and the source weighs 3.43 kg (7.6 lb).

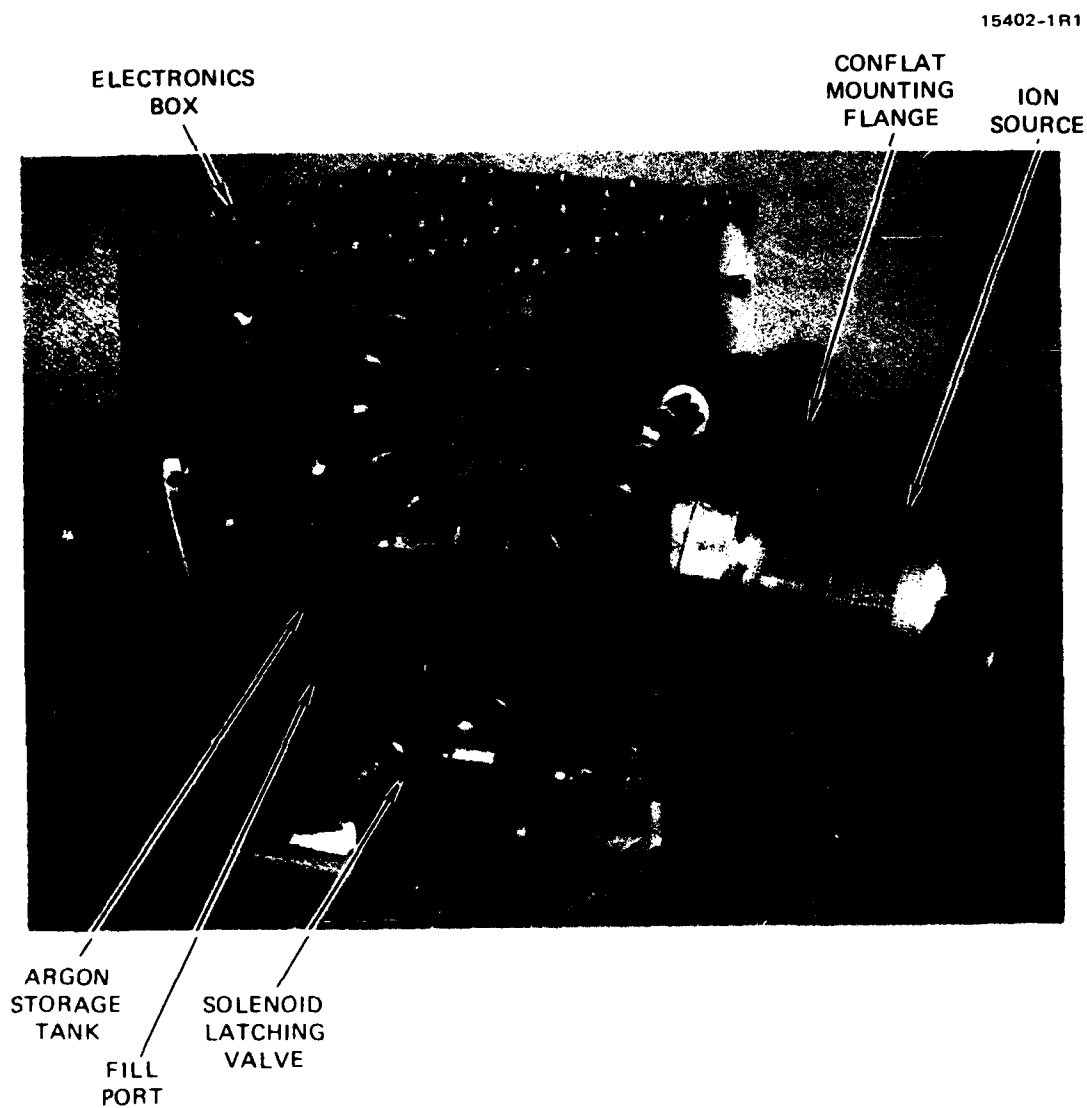


Figure 2-1. Flight-model PIES mounted on a test fixture.

Table 2-1. Positive Ion Ejection System Specifications

15479-44

PARAMETER	SPECIFICATION
EJECTED CURRENT DYNAMIC RANGE	TWENTY μ A TO TWENTY mA.
EJECTED CURRENT SET POINTS	SETTABLE TO SIXTEEN LEVELS, INCLUDING ZERO, TWENTY μ A AND TWENTY mA, IN A QUASI-LOGARITHMIC FASHION. THE ADJACENT NON-ZERO LEVELS HAVE A RATIO OF $\approx 1.64:1$. THESE LEVELS ARE COMMANDED EXTERNALLY BY MEANS OF FOUR BITS OF AN EIGHT-BIT PARALLEL DIGITAL BUS.
EXPELLANT TYPE	ARGON GAS.
ENERGY DYNAMIC RANGE	0.5 TO 4.5 keV.
ENERGY DISTRIBUTION	90% OF THE BEAM IONS HAVE AN ENERGY WITHIN 10% OF THE SET ENERGY VALUE.
ENERGY SET POINTS	SETTABLE TO 0.5, 2.0, AND 4.5 keV, USING TWO OF THE EIGHT BITS OF THE PARALLEL DIGITAL COMMAND BUS.
COMMAND RATE	ADJACENT COMMAND NUMBER SET COMMANDS OCCUR NO FASTER THAN ONE EVERY TWENTY ms. 50-ms DELAYS ARE INSERTED AT EVERY ENERGY LEVEL CHANGE TO ALLOW FOR POWER SUPPLY SETTLING.
COMMAND INTERFACE	THE SYSTEM ACCEPTS AND LATCHES COMMANDS VIA A PARALLEL EIGHT-BIT DIGITAL DATA BUS AND DATA-LATCH LINE. SIGNAL LEVELS ARE TTL COMPATIBLE.
LIFETIME - WITHOUT REPLACEABLE PARTS (FLIGHT MODEL)	TWENTY HOURS PLUS TWENTY MINUTES FLIGHT INCLUDING LAUNCH ENVIRONMENT.
LIFETIME - WITH REPLACEABLE PARTS	ONE HUNDRED HOURS LABORATORY TESTING.
SIZE (FLIGHT MODEL)	FITS INTO A CYLINDER OF LESS THAN 43.2 cm (17 in.) IN DIAMETER AND 30.5 cm (12 in.) IN LENGTH.
ELECTRONICS	THE SYSTEM INCLUDES COMPLETE ELECTRONICS FOR POWER PROCESSING AND INSTRUMENT CONTROL FOR BOTH FLIGHT OPERATIONS AND GROUND TESTS.

Table 2-1. Continued

15479-45

PARAMETER	SPECIFICATION
POWER	SYSTEM OPERATES FROM A 28 ± 4 V SUPPLY. PEAK POWER IS LESS THAN 245 W.
EXPELLANT STORAGE AND DISPENSING	STORAGE TANK WITH SUFFICIENT GAS FOR AT LEAST FOUR HOURS OF OPERATION; GAS VALVE, AND GAS FLOW REGULATOR ARE INCLUDED IN THE SYSTEM.
CONSTRUCTION	A VACUUM INTERFACE, ALLOWING THE ELECTRONICS TO OPERATE AT ONE ATMOSPHERE WHILE THE SOURCE OPERATES AT VACUUM, IS PROVIDED.
START-UP	THE ION BEAM EJECTION SYSTEM CAN BE OPERATED AT FULL CAPABILITY WITHIN 100 SECONDS AFTER ROCKET LAUNCH.
OUTPUT SIGNALS	ANALOG OUTPUTS ARE IN THE RANGE OF 0 TO +5.1 VOLTS AND INCLUDE TOTAL POSITIVE ION CURRENT, BEAM ENERGY, AND SYSTEM DIAGNOSTICS. SYSTEM STATUS VERIFICATION OF INPUT COMMANDS IS VIA TTL COMPATIBLE DIGITAL SIGNALS.
WEIGHT (FLIGHT MODEL)	LESS THAN 11 kg (24.2 lbs).
SURVIVABILITY (FLIGHT MODEL)	WILL SURVIVE AND OPERATE WITHIN SPECIFICATION AFTER LAUNCH ON A NIKE-BLACK BRANT V ROCKET.
VIBRATION (3 AXIS)	SINE: ± 1 g, 20 TO 2000 Hz, 3 OCTAVES PER MINUTE. RANDOM: $0.1 \text{ g}^2/\text{Hz}$, 100 TO 1000 Hz WITH A 6 dB PER OCTAVE ROLLOFF FROM 100 TO 20 Hz AND 1000 TO 2000 Hz.
SHOCK (3 AXIS)	TRANSIENT: 50 g, 1/2 SINE, 11 ms.
THERMAL-VACUUM	THE SYSTEM FUNCTIONS WITHIN SPECIFICATIONS FROM -10°C TO 50°C AT ATMOSPHERIC PRESSURE. THE SYSTEM WILL SURVIVE TEMPERATURES OF -24°C TO 61°C .

SECTION 3

ION SOURCE

The ion source developed for PIES is a modified SIT-5 ion thruster that was developed for NASA's Lewis Research Center by Hughes. It consists of an ion-optics assembly, a discharge chamber (with integral magnets and magnetic polepieces), a filamentary cathode-assembly, and a high-voltage isolator (see Figure 3-1). The major modifications from a SIT-5 thruster are replacement of the two-grid extraction system with a three-grid system, replacement of the hollow cathode with a filament, and elimination of the neutralizer.

3.1 MECHANICAL DESIGN

The ion-optics assembly shown in Figure 3-2 consists of three molybdenum grids. The grids are fabricated from 0.020-in.-thick arc-cast molybdenum sheets that are match drilled to form the 207 beam-forming apertures. The apertures are in a hexagonal pattern on 0.30-cm (0.118-in.) centers. The details of the geometry of each beam-forming aperture are shown in Figure 3-3. The first grid (screen electrode) is 8 sided and is mounted directly to the discharge chamber. The second and third grids (accel and decel electrodes, respectively) are square and are supported at their corners by high-voltage standoff insulators. The insulators are vented internally to permit rapid evacuation and thus avoid Paschen breakdown.

The discharge chamber consists of a thin, ribbed shell which is terminated at each end by magnetic iron polepieces. The polepieces are connected by eight brazed tubes which house Alnico-V permanent magnets. A thin, ribbed anode is supported inside the discharge chamber by four standoff insulators.

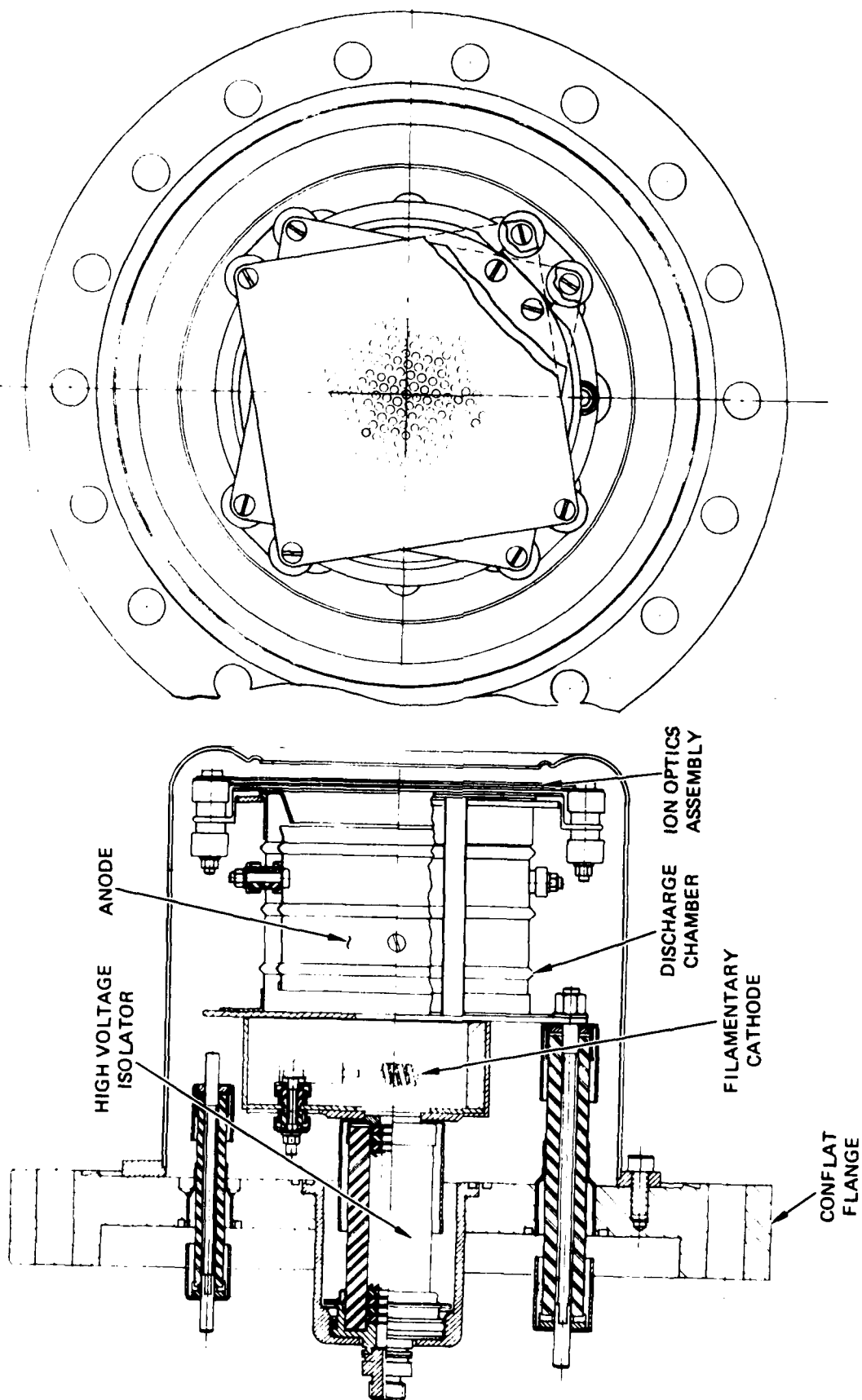


Figure 3-1. PIES ion source assembly.

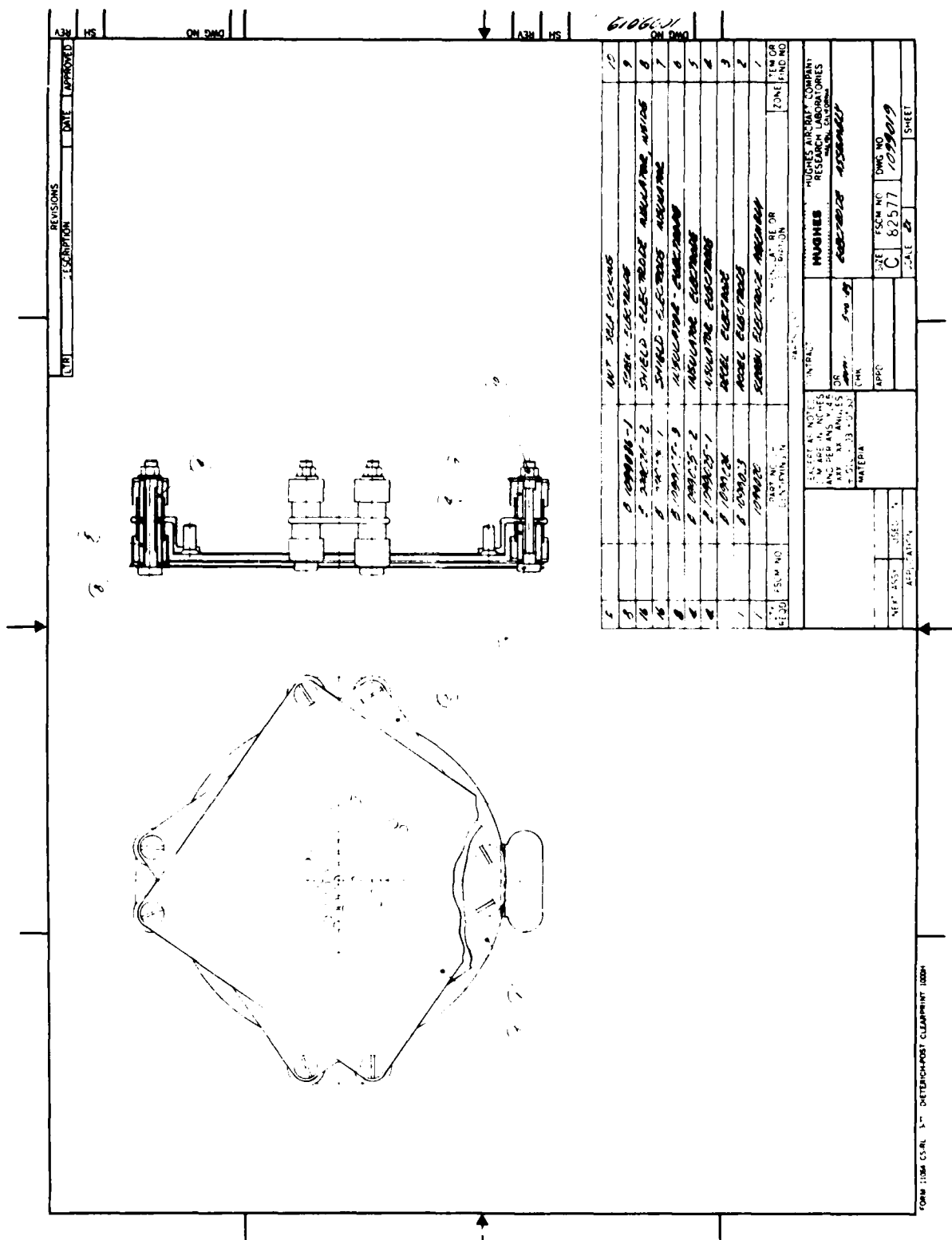
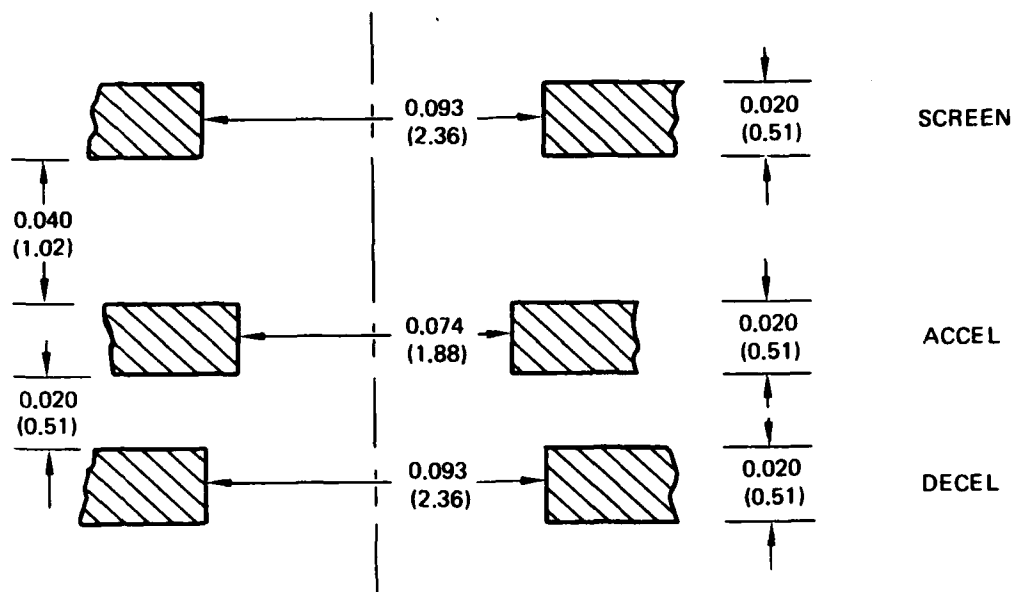


Figure 3-2. Ion optics assembly.



DIMENSIONS ARE IN INCHES (mm)

Figure 3-3. Details of each beam forming aperture.

The spiral-wound filamentary cathode is made of thoriated tungsten. The thoriated tungsten material permits ground operation of the ion source without loss of filament ductility that is essential for the filament to withstand the launch environment. A second filament (which is never operated on the ground) is provided as a backup to the primary filament. The two filaments are mounted side by side and slightly off-axis in a slide-out cassette for ease of filament replacement.

The high-voltage isolator provides electrical isolation of the filamentary cathode and discharge chamber from the system chassis, while accomodating the flow of argon expellant. Paschen breakdown of the argon gas is avoided by separating the total potential difference, which appears across the isolator (up to 4500 V), into many smaller voltages (each less than that required for Paschen breakdown). The isolator consists of an alumina cylinder, the interior of which is filled with wire-mesh screens separated by ceramic washers. This design assures that the mesh-to-mesh potential difference is less than the Paschen breakdown voltage at the worst-case pressure-distance product. The isolator is held in compression by the mounting structure, taking advantage of the very high compressive strength of alumina.

The ion source is mounted on a 6.75-in.-diameter "Conflat" flange with welded-in-place ceramic insulators, providing a vacuum interface for testing and flight purposes. Ceramic insulators are able to withstand the launch environment because they are held in compression by the mounting bolts.

3.2 FILAMENT TESTS

Filaments of tungsten, thoriated tungsten, and tantalum-yttrium were tested for use in this application. The filaments were operated in vacuum and were powered by a laboratory constant-current power supply that exhibits approximately 50% overshoot on power-up. (This overshoot characteristic is similar

to that of the flight filament power supply.) A microcomputer was programmed to turn the filament power supply ON for one minute and OFF for one minute on a continuous basis. The microcomputer recorded the equilibrium filament voltage (at the same current value) at the end of each cycle, and printed out a five-cycle average of this voltage. A shorted or open filament was detected by abnormally low or high filament voltage, respectively. Facility pressure was monitored by reference to the ionization-gauge controller output. Any of these faults (shorted or open filament or high facility pressure) caused the test to be interrupted and a fault message to be printed.

We performed three separate filament tests using this facility: a spiral tungsten filament, a spiral Ta:Y filament, and a hairpin Ta:Y filament. The tungsten spiral filament shorted after 970 cycles (16.2 h on-time) and exhibited extreme brittleness when removed. The Ta:Y spiral filament shorted after 5400 cycles (90 h on-time), but still exhibited great ductility when removed. The Ta:Y hairpin filament broke after 7700 cycles (128 h on-time) and exhibited substantial brittleness when removed (attributed to the loss of yttrium by evaporation).

From these tests we concluded that:

- the excessive brittleness of pure tungsten filaments provides little confidence in their ability to withstand launch vibration following ground testing;
- Ta:Y filaments are highly ductile until near the end of life, at which time evaporation loss of yttrium produces brittleness;
- spiral-wound filaments have a significant tendency to short unless they are properly stress-relieved and are mounted in an unstressed condition.

As a result of these tests, Ta:Y was our first choice for filament material; however, problems with delivery of Ta:Y filaments forced us to try thoriated-tungsten in order to start testing of the breadboard system. The thoriated-tungsten

filaments were still ductile after operation in the breadboard and were put through vibration testing by AFGL and survived. Because thoriated-tungsten was adequate to meet the requirements of the program, Ta:Y was dropped even though it was our first choice.

The flight source performed reliably throughout the testing of the flight system. However, when the filaments were replaced just prior to delivery of the hardware, it was discovered that both filaments in the source were partially shorted and evidently had been shorted throughout the testing. Figure 3-4(a) shows the original design of the filaments and the approximate location of the short. Approximately 75% of the filament was shorted out in both cases and did not produce any emission; therefore, it was concluded that only 25% of the original filament length was needed to produce the required emission.

The simplified filament design which has only 25% of the original length is shown in Figure 3-4(b). Three filaments of this type were tested in the flight source; they were found to be compatible with the electronics and produced the same test results as the shorted filaments of the original design. It is very unlikely that the simplified design will ever short out, and it should perform better during vibration because of lower cantilevered mass. The flight source was delivered with filaments of the simplified design.

3.3 CHARGE EXCHANGE

Argon ions leaving PIES undergo charge-exchange (CX) collisions with argon neutrals leaving the source (and to a lesser extent, with other neutrals emanating from the rocket and associated particle sources). In the CX process, fast beam ions become atomically neutralized, and slow neutrals become ionized.

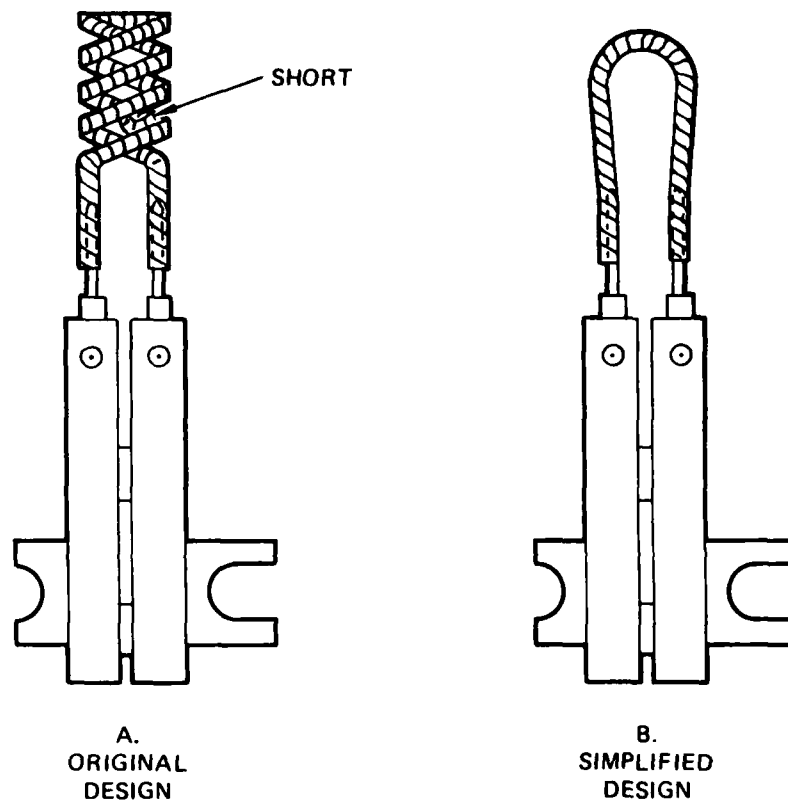


Figure 3-4. Original and simplified filament designs on their mounting brackets.

The CX process has the undesirable effect of (1) reducing the true beam current leaving the rocket, and (2) producing a low-energy ion population near the rocket. These low-energy ions will be formed at a potential that is somewhere between rocket potential and space potential. A simple calculation was performed to determine the level of charge exchange expected in the ion beam. This calculation (which follows) shows a worst case value for the CX fraction of 8.3%

The charge-exchange current produced in the ion beam is given by the equation,

$$I_{CX} = n_0 n_+ e \sigma_{CX} v_+ V \quad , \quad (1)$$

where

I_{CX} is the charge-exchange current,
 n_0 is the neutral-species density,
 n_+ is the argon-beam-ion density,
 σ_{CX} is the cross-section for charge exchange,
 v_+ is the argon-beam-ion velocity,
 V is the interaction volume, and
 e is the electronic charge.

The ion-beam current leaving PIES can be expressed as

$$I_+ = n_+ e v_+ A \quad , \quad (2)$$

where A is the ion-beam cross-sectional area. Equations (1) and (2) are readily combined to yield

$$\frac{I_{CX}}{I_+} = \frac{n_0 \sigma_{CX} V}{A} \quad . \quad (3)$$

The charge-exchange-interaction volume, V , in Equation (3) can be taken to be a volume which has a cross-sectional area equal to that of the ion beam and extending a characteristic distance away from the ion source. This characteristic distance is the distance over which charge-exchange phenomena are of importance to the BERT-I experiment; charge exchange occurring outside the Debye sheath that surrounds the rocket will have no effect on the rocket charging properties. The thickness of this sheath for the range of anticipated plasma parameters (plasma density of 10^{10} to 10^{11} m^{-3} at electron temperatures of 0.2 to 1 eV) turns out to be less than one PIES beam diameter (50 mm). If the Debye sheath was in fact much thicker than this, the calculated charge exchange current would not be much different because the neutral density falls off rapidly away from the PIES, with a scale length equal to the beam diameter.

We modeled the interaction volume by (conservatively) assuming the neutral density to be constant throughout a volume which coincides with the ion-beam diameter and is one beam-diameter deep. The neutral density can be found from the equation,

$$I_0 = n_0 v_0 e A / 4 \quad , \quad (4)$$

where v_0 is the neutral-argon particle velocity, and I_0 is the total neutral argon flowrate into the ion source. (This is a conservative assumption, since the neutral flow leaving the source is reduced by the amount of the ion-beam current.) Using Equation (3) and (4) and a value of the cross-section, σ_{CX} , corresponding to the worst-case beam energy, we find a result of

$$I_{CX}/I_+ = 0.083 \quad .$$

Thus, under the conservative and worst-case assumptions given above, we conclude that <8.3% of the ion-beam current will be lost to charge exchange before the beam is one space Debye length from the rocket. The values of the constants we used in the calculation are:

$$\sigma_{cx} = 2.5 \times 10^{-19} \text{ m}^2 \text{ (at } V_B = 4.5 \text{ keV)}$$

$$I_0 = 96 \text{ mA equivalent (1 SCCM)}$$

$$V_0 = 350 \text{ m/s}$$

$$A = 1.03 \times 10^{-3} \text{ m}^2$$

$$V = 51.6 \times 10^{-6} \text{ m}^3$$

$$e = 1.602 \times 10^{-19} \text{ C.}$$

SECTION 4

POWER ELECTRONICS UNIT (PEU)

The power electronics unit (PEU) contains the four power supplies (filament, discharge, accel, and screen) required to operate the ion source, a housekeeping inverter, a log electrometer to measure the net ion current expelled from the source, and the command and telemetry interfaces. The following sections discuss these elements.

4.1 FLYBACK INVERTERS

All of the power supplies or inverters used for PIES are of the flyback topology (see Figure 4-1) which provides isolation and high reliability while requiring a minimum number of components. Only four power-handling components are required:

- one transformer (T1)
- one transistor switch (Q1)
- one blocking diode (CR1)
- one filter capacitor (C1).

Since operation is in a current-source mode rather than a voltage-source mode, flyback topology exhibits inherent short-circuit protection. The flyback inverter functions by cyclically storing energy in the magnetic field of transformer T1 while Q1 is turned ON. This stored energy is then transferred to T1's secondary and through diode CR1 to the output filter (C1) and the load when Q1 is OFF. By varying the Q1 ON time, the amount of energy stored and transferred to the load in each cycle can be controlled or regulated in proportion to changes in input voltage, output load, or commanded setpoint.

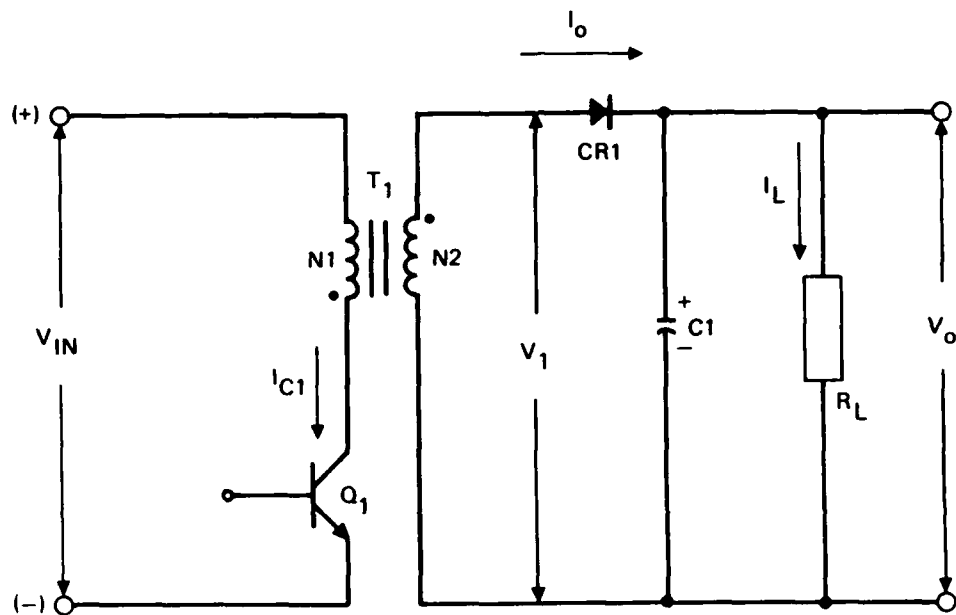


Figure 4-1. Simplified schematic of a half-wave flyback inverter.

4.2 FILAMENT SUPPLY

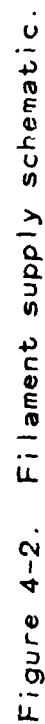
The filament supply is shown schematically in Figure 4-2. The supply produces a maximum output of 16 V at 7 A and is controlled by an integrated circuit (U1) which is a pulse-width-modulator (PWM). Regulation is accomplished by monitoring (T2) and controlling the flyback-inverter-primary peak current, rather than the output current. By using this approach, the output power is regulated (rather than the output current) with a linear control-voltage to output-power transfer function. This regulation approach is implemented with simple circuitry (on the primary side of the inverter) in the face of the highly nonlinear load characteristics that result from filament temperature variations.

Optical isolation (U2) is provided to isolate the control circuitry from input-power ground. This was found to be necessary in order to eliminate noise problems in the control circuitry. The input power, command/telemetry, and output grounds are all isolated from each other by transformers and/or optical couplers.

The voltage telemetry is derived from a separate winding on the output transformer (T1). A synchronous sample-hold circuit (Q5) is used to minimize the effects of the leading-edge-transient spike. This telemetry voltage is also fed back to the PWM to limit the output voltage under open-circuit conditions.

The current telemetry is derived from a current transformer (T3) in the secondary of the output transformer. The signal from T3 is rectified and then integrated by U3 to provide the telemetry signal.

Switching between the two filaments in the source is automatically accomplished by Q7 and Q8. If the main filament breaks, then the output voltage will rise high enough to turn Q8 ON via VR6. Q8 turns Q7 ON, applying power to the second filament and latching Q8 (and hence Q7) ON via VR7.



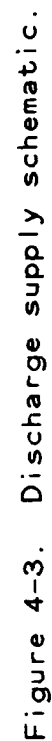
4.3 DISCHARGE SUPPLY

The discharge-supply design shown in Figure 4-3 is a half-wave flyback inverter which produces a maximum output of 60 V at 0.5 A and 180 V under open-circuit conditions. The polypropylene output capacitor has a series equivalent resistance of approximately 10 m Ω which allows meeting the 1% ripple specification with a half-wave circuit instead of a full-wave circuit. Voltage regulation is provided by sensing and comparing the output voltage directly with a TL431 shunt regulator (Q6). The error signal from Q6 drives an optical coupler (U2), which in turn controls the PWM (U1). Under light load conditions the output from U4 via R44, CR9, CR10, and CR11 alters the voltage feedback and allows the output to rise to 180 V. The output voltage-current characteristic of this supply is shown in Figure 4-4.

Primary-side overcurrent protection is provided by sensing the primary peak current (T2) and limiting this current to a value approximately 20% higher than that required to deliver the 30-W output power. Output peak-current limiting is provided by feeding the current telemetry signal back to the PWM via CR12.

4.4 ACCEL SUPPLY

The accel supply has a maximum output of 500 V at 5 mA and is shown in Figure 4-5. The output voltage is regulated by sensing it with a separate winding on the output transformer (T1) and feeding this signal back to the error amplifier in the PWM (U1). R35 is in series with the output to limit transient currents and noise if arcs occur between the extraction grids on the ion source.



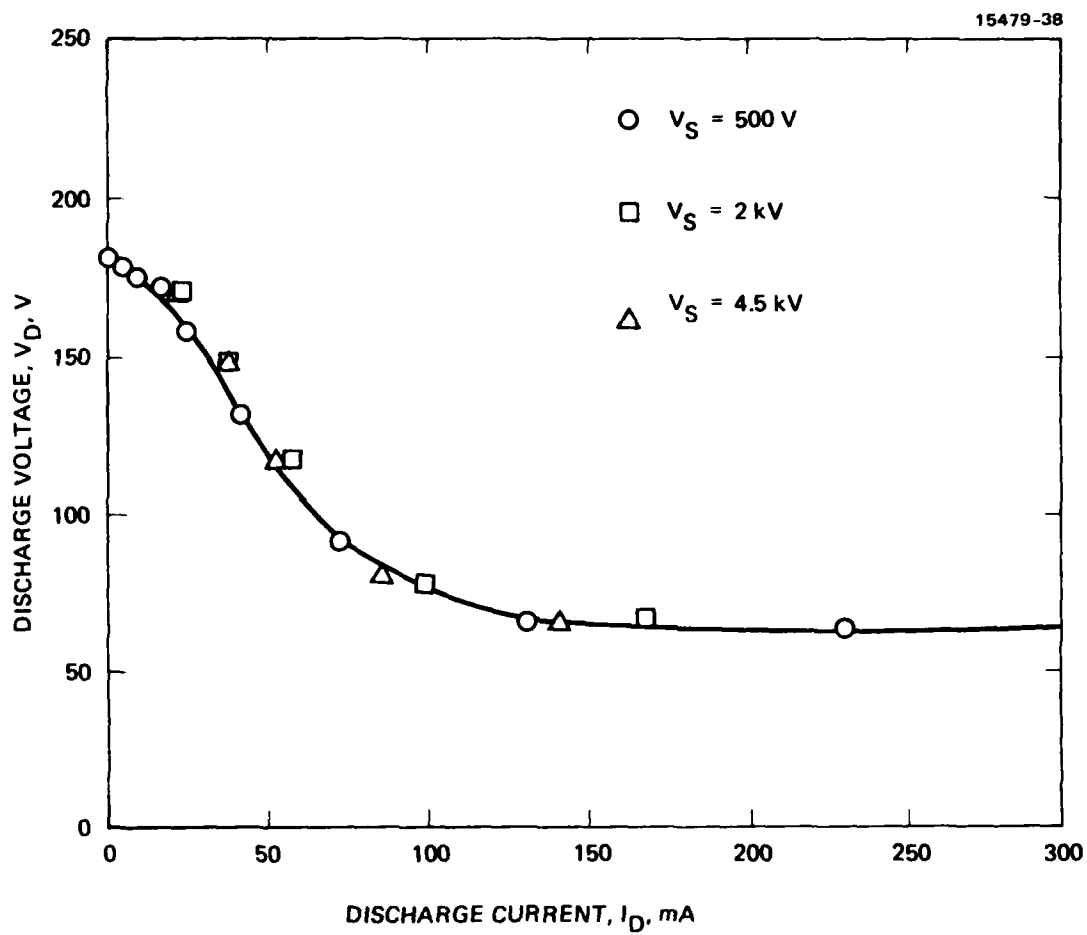


Figure 4-4. Output voltage-current characteristic of the discharge supply.

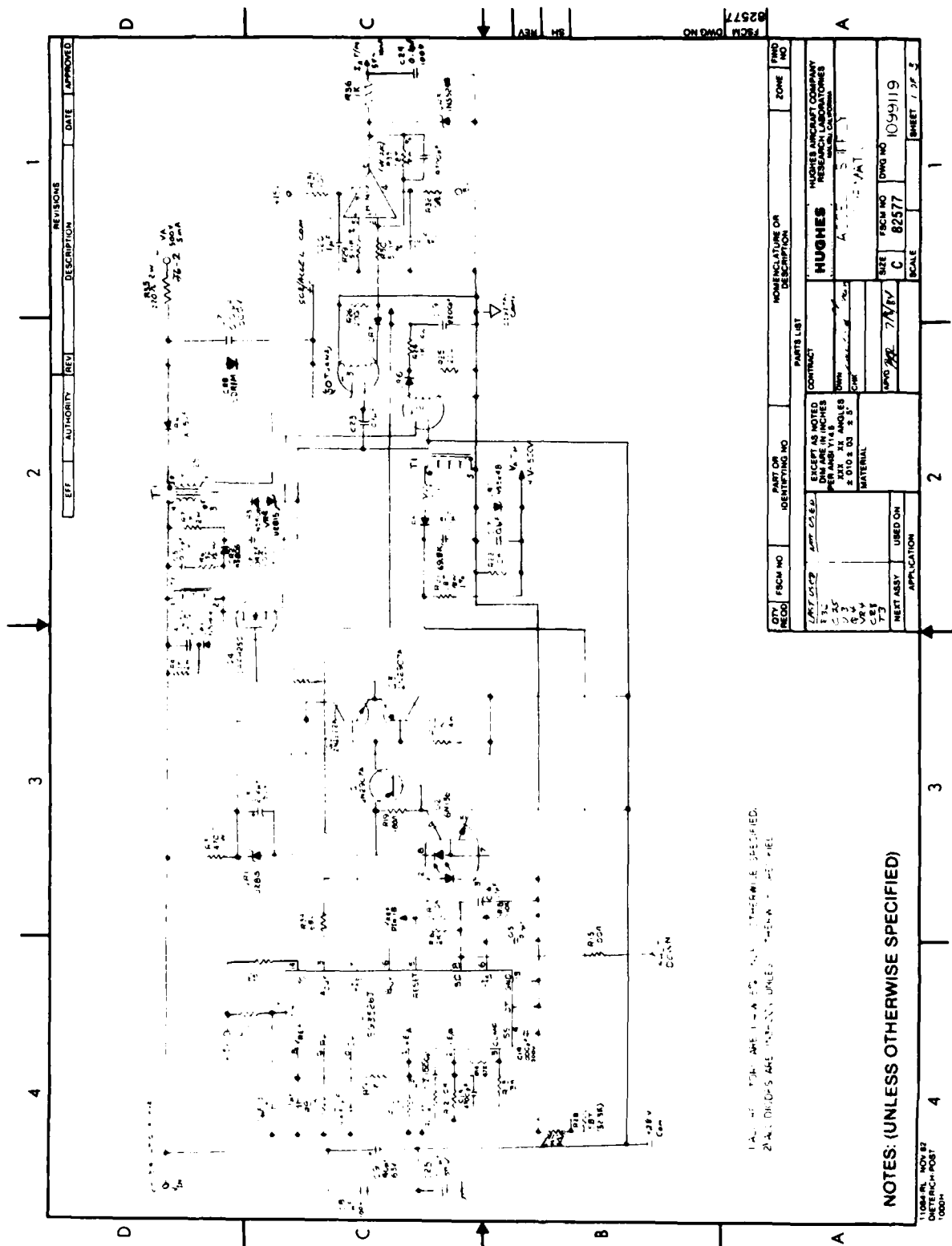


Figure 4-5. Accel supply schematic.

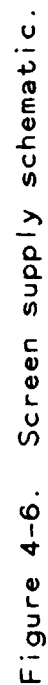
4.5 SCREEN SUPPLY

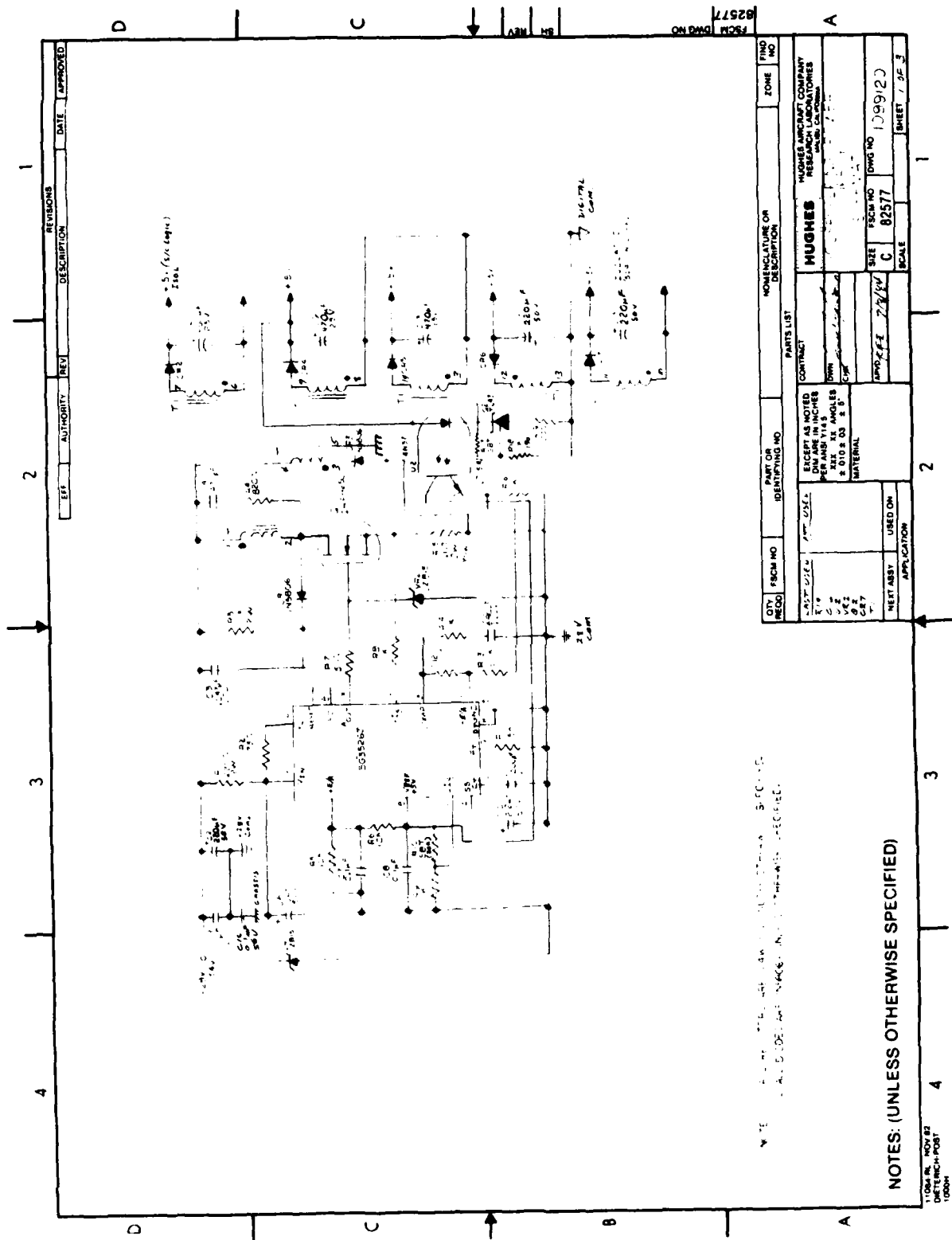
The screen supply shown in Figure 4-6 produces outputs of 0.5, 2.0, and 4.5 kV at 0 to 25 mA. It can best be described as a resonant flyback inverter consisting of two separate, alternate-phase inverters feeding a single output. The reflected capacitance to the primaries of the high voltage secondary windings (T1 and T2) causes high transient currents in the MOSFET switches if the transformers are driven by a standard push-pull configuration. By incorporating this otherwise detrimental capacitance into a tuned resonant circuit, the MOSFET switches (Q4 and Q8) can be turned OFF at near-zero voltage and ON at near-zero current. This design minimizes power-switch losses and enables operation at considerably higher frequencies than with push-pull configurations by using two output transformers (T1 and T2) instead of one.

The output voltage is sensed directly with a high frequency (500-kHz) amplitude-modulated sense circuit (U5, U6, Q10, Q11, T3, T4, and Q9). The signal from the synchronous rectifier (Q9) is fed back to the error amplifier of the PWM (U1). The voltage telemetry is derived from this same signal and the current telemetry is obtained by sensing the output current (T7 and U4). R9 through R12 are in series with the output to limit transient currents and noise if the extraction grids on the ion source should arc.

4.6 HOUSEKEEPING INVERTER

The housekeeping-inverter design, shown in Figure 4-7, employs the same basic single-MOSFET flyback circuit used for the supplies described above. The inherent simplicity of the flyback configuration for multiple-output use is apparent, as shown by the five separate, regulated outputs which require only a diode and capacitor for each output. Regulation of all outputs requires that only the most critical output (the 5-V logic output in this case) be sensed and regulated. Overcurrent protection is provided by monitoring the MOSFET current with a 0.1- Ω resistor (R15).





NOTE: ALL COMPONENTS ARE TO BE SPECIFIED BY THE USER. THE USER IS RESPONSIBLE FOR THE PROPER SELECTION OF COMPONENTS.

NOTES: (UNLESS OTHERWISE SPECIFIED)

1100V AC, 60 HZ
DETRENCH-POST
1000H

QTY REQD	FSCM NO	PART OR IDENTIFYING NO	NOMENCLATURE OR DESCRIPTION	ZONE	FIND NO														
<table border="1"> <tr> <td colspan="2">PARTS LIST</td> </tr> <tr> <td>SECRET AS NOTED BY THE USER PER ANSI Y14.5 EXC. 10 ANGLES UNLESS OTHERWISE SPECIFIED</td> <td>CONTRACT</td> </tr> <tr> <td colspan="2">HUGHES AIRCRAFT COMPANY RESEARCH LABORATORIES 3801 UNIVERSITY AVENUE SANTA MONICA, CALIF. 90405</td> </tr> <tr> <td>SIZE</td> <td>FSCM NO</td> </tr> <tr> <td>C</td> <td>82577</td> </tr> <tr> <td>SCALE</td> <td>1099/20</td> </tr> <tr> <td colspan="2">SHEET 1 OF 3</td> </tr> </table>						PARTS LIST		SECRET AS NOTED BY THE USER PER ANSI Y14.5 EXC. 10 ANGLES UNLESS OTHERWISE SPECIFIED	CONTRACT	HUGHES AIRCRAFT COMPANY RESEARCH LABORATORIES 3801 UNIVERSITY AVENUE SANTA MONICA, CALIF. 90405		SIZE	FSCM NO	C	82577	SCALE	1099/20	SHEET 1 OF 3	
PARTS LIST																			
SECRET AS NOTED BY THE USER PER ANSI Y14.5 EXC. 10 ANGLES UNLESS OTHERWISE SPECIFIED	CONTRACT																		
HUGHES AIRCRAFT COMPANY RESEARCH LABORATORIES 3801 UNIVERSITY AVENUE SANTA MONICA, CALIF. 90405																			
SIZE	FSCM NO																		
C	82577																		
SCALE	1099/20																		
SHEET 1 OF 3																			

Figure 4-7. Housekeeping inverter schematic.

4.7 LOG ELECTROMETER

The schematic of the log electrometer which measures the ejected ion current is shown as part of Figure 4-8. The 0 to 5-V analog output covers the input current range of 1 μ A to 25 mA. The base-emitter junction of a transistor (Q1A) in the feedback loop of an operational amplifier (AR4) is used to compute the log of the input current. Q2 adds current gain to the output of AR4 since it cannot supply the 25 mA. Temperature compensation of the circuit is accomplished with Q1B and R77 which null out the drifts associated with Q1A. The constant-current source, Q3, sets the low end of the current range (1 μ A) and R18 sets the high end of the current range (25 mA). The circuit was tested over a temperature range of 25 to 80°C and drifts less than 0.02% of full scale output voltage per °C. The calibration curve for the flight log electrometer is presented in Figure 4-9.

4.8 COMMAND AND TELEMETRY INTERFACE

All commands required to operate the PIES are contained in one 8-bit parallel TTL-compatible digital word. The format of this word is shown in Table 4-1. Bit 0 is used to control the gas valve, bit 1 turns the four power supplies ON or OFF, bits 2 and 3 control the beam energy, and bits 4 through 7 control the emission current.

This 8-bit word is optically isolated at the input to the PEU (U6 through U14 of Figure 4-10) and stored in an 8-bit latch (U15 and U16). The output of the latch is buffered (U26 through U28) and optically isolated (U18 through U25) to provide a TTL-compatible telemetry signal of what is stored in the latch. The telemetry signal can be read out as a parallel word (from U5) or as a serial word (via U3 and U4). U30 and U31 of Figure 4-10 provide the analog reference signal for the emission current feedback loop, and U32 provides the analog reference signal for the screen supply (beam energy).

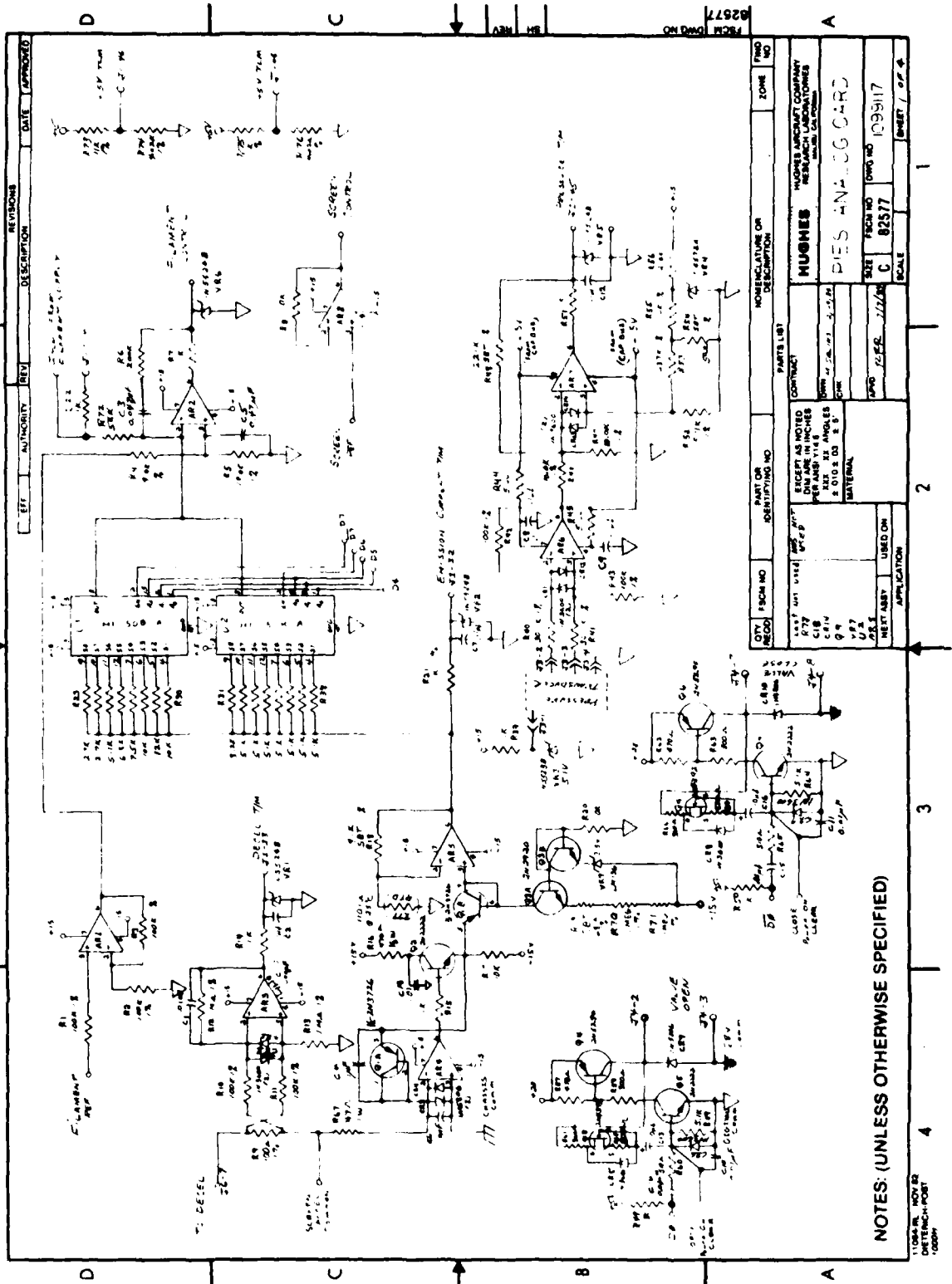


Figure 4-8. Analog control circuitry schematic.

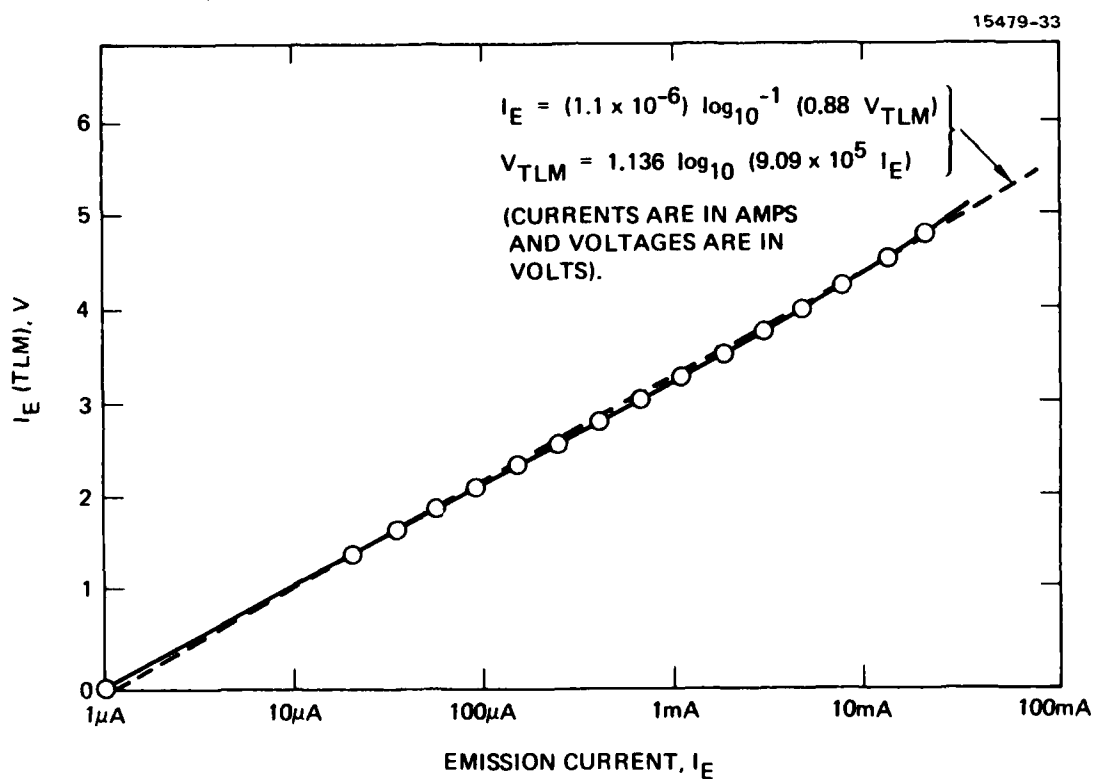


Figure 4-9. Calibration curve for the flight log electrometer.

Table 4-1. Command Word Format

15479 32

BITS								FUNCTION	
7	6	5	4	3	2	1	0		
X	X	X	X	X	X	X	0	VALVE CLOSED	
X	X	X	X	X	X	X	1	VALVE OPEN	
X	X	X	X	X	X	0	X	SOURCE OFF	
X	X	X	X	X	X	1	X	SOURCE ON	
X	X	X	X	0	0	X	X	}	BEAM ENERGY
X	X	X	X	0	1	X	X		
X	X	X	X	1	0	X	X		
X	X	X	X	1	1	X	X		
0	0	0	0	X	X	X	X	}	EJECTED CURRENT
0	0	0	1	X	X	X	X		
0	0	1	0	X	X	X	X		
0	0	1	1	X	X	X	X		
0	1	0	0	X	X	X	X		
0	1	0	1	X	X	X	X		
0	1	1	0	X	X	X	X		
0	1	1	1	X	X	X	X		
1	0	0	0	X	X	X	X		
1	0	0	1	X	X	X	X		
1	0	1	0	X	X	X	X		
1	0	1	1	X	X	X	X		
1	1	0	0	X	X	X	X		
1	1	0	1	X	X	X	X		
1	1	1	0	X	X	X	X		
1	1	1	1	X	X	X	X		

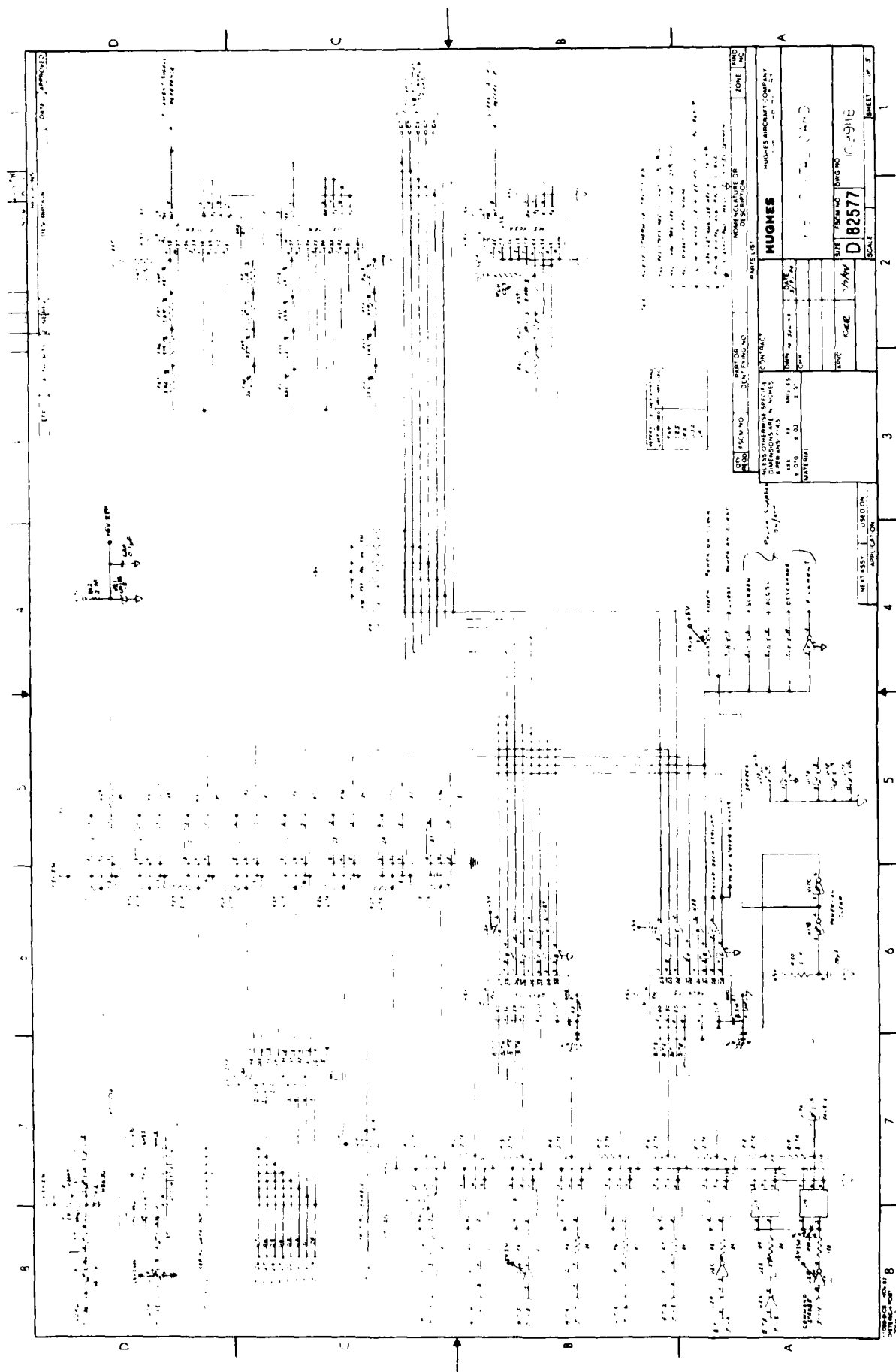


Figure 4-10. Digital control circuitry schematic.

The analog control circuitry for PIES (Figure 4-8) consists of the emission-current feedback loop (AR1, U1, U2 and AR2), the decel current, TLM (AR3), the emission-current log electrometer (AR4, Q1, Q2, Q3, and AR5), the valve drivers (Q4 through Q7), the screen-control buffer (AR8), and the pressure-transducer signal conditioning (AR6 and AR7). A complete list of the PIES analog TLM is given in Table 4-2.

Table 4-2. PIES Analog Telemetry Signals

15479-30

PARAMETER	RANGE	ACCURACY, %
DISCHARGE VOLTAGE	0 TO 250 V	5
DISCHARGE CURRENT	0 TO 1 A	5
FILAMENT VOLTAGE	0 TO 18 V	5
FILAMENT CURRENT	0 TO 10 A	5
ACCEL VOLTAGE	0 TO 640 V	5
ACCEL CURRENT	0 TO 4 mA	5
SCREEN VOLTAGE	0 TO 5 kV	5
SCREEN CURRENT	0 TO 30 mA	5
ION BEAM CURRENT	1 μ A TO 25 mA (LOGARITHMIC)	5
DECEL CURRENT	0 TO 5 mA	5
+5V	0 TO 6.25 V	5
+15V	0 TO 18.75 V	5
GAS RESERVOIR PRESSURE	0 TO 500 PSIA	5

SECTION 5

EXPELLANT FEED SYSTEM

The expellant storage and feed system for PIES consists of a storage tank, fill valve, flow impedance, pressure transducer, and latching solenoid valve. The configuration of these components is shown in Figure 5-1.

The cylindrical storage tank is 9.0 cm (3.6 in.) in diameter and 13.2 cm (5.25 in.) long. It has a single port on one end (per MS 33649-6) and the closed end is elliptical. Its volume is 0.492 l (30 in.³) and is rated for operation at 3000 psi. The tank is tested at 5000 psi and is DoT-qualified per specification 3HT3000. It is fabricated of Type 4130 steel and has a mass of less than 0.91 kg (2 lb). Corrosion and oxidation resistance are provided by paint on the outside and by an inside coating.

The outlet port is fitted with an O-ring-sealed header (per MS 24385-6) that provides a boss for the fill fitting (MS 28889), the pressure transducer (Entran Devices Model EPS-1032-1000), and the flow impedance. A latching solenoid valve is located directly downstream of this header to control (ON/OFF) the flow of argon to the source. The valve is a mechanical latching type of valve and is manufactured by Futurecraft, City of Industry, CA (Model 200487). The mechanical latching feature is acceptable for this application because of the low number of cycles required (<1000).

Flow regulation is provided by a fixed flow impedance which is driven by a relatively constant pressure of xenon gas in the storage tank over the length of the flight (approximately 8 min). The fixed flow impedance is a porus-tungsten plug. Porus metal offers the advantage of multiple, interlaced flow channels, so that the flowrate is essentially unaffected if the plug becomes partially occluded by debris.

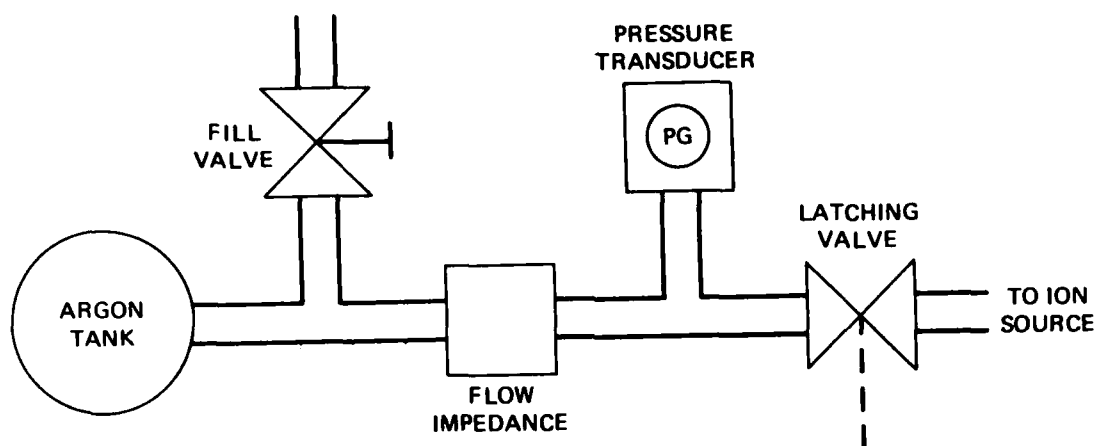


Figure 5-1. Expellant feed system configuration.

The porous-tungsten flow impedance was calibrated for flowrate versus gas pressure. This calibration is shown in Figure 5-2, along with an ideal curve that was normalized at 200 psia and 1.1 SCCM. These are the pressure and flowrate at which the system is operated. The ideal curve was calculated for the flowrate being proportional to $(P_1)^2 - (P_2)^2$ where P_1 is the gas pressure in the expellant tank and P_2 is zero (vacuum). The data are a good fit to this type of curve.

The time required to fill the ullage volume between the porous-tungsten flow impedance and the valve (Figure 5-1) was measured and the data are presented in Figure 5-3. The data are a good fit to an exponential curve, with a time constant of 17 min. The pressure transducer is located in this ullage volume; therefore, the gas valve must have been closed for at least an hour in order to obtain an accurate reading of the pressure in the expellant tank. The pressure transducer is in the ullage volume so that it can be used as an indicator that the valve has opened (pressure drops to zero when the valve opens).

An estimate of the operating time of the system was made assuming that the tank was initially filled to 200 psia. The cutoff point below which operation of the ion source becomes questionable is 0.75 SCCM. From Figure 5-3 this corresponds to 165 psia. If the flow rate is assumed to average 1 SCCM over the pressure range of 200 psia down to 165 psia, then a conservative estimate of operating time is obtained. The expellant tank has a volume of 0.5 liters 6.8 standard liters of gas when filled to 200 psia and 5.6 standard liters when filled to 165 psia. This gives a usable gas volume of 1.2 standard liters or 1200 standard cubic centimeters. At a flowrate of 1 SCCM or 60 scc/h, it will be 20 h before the usable gas volume is consumed.

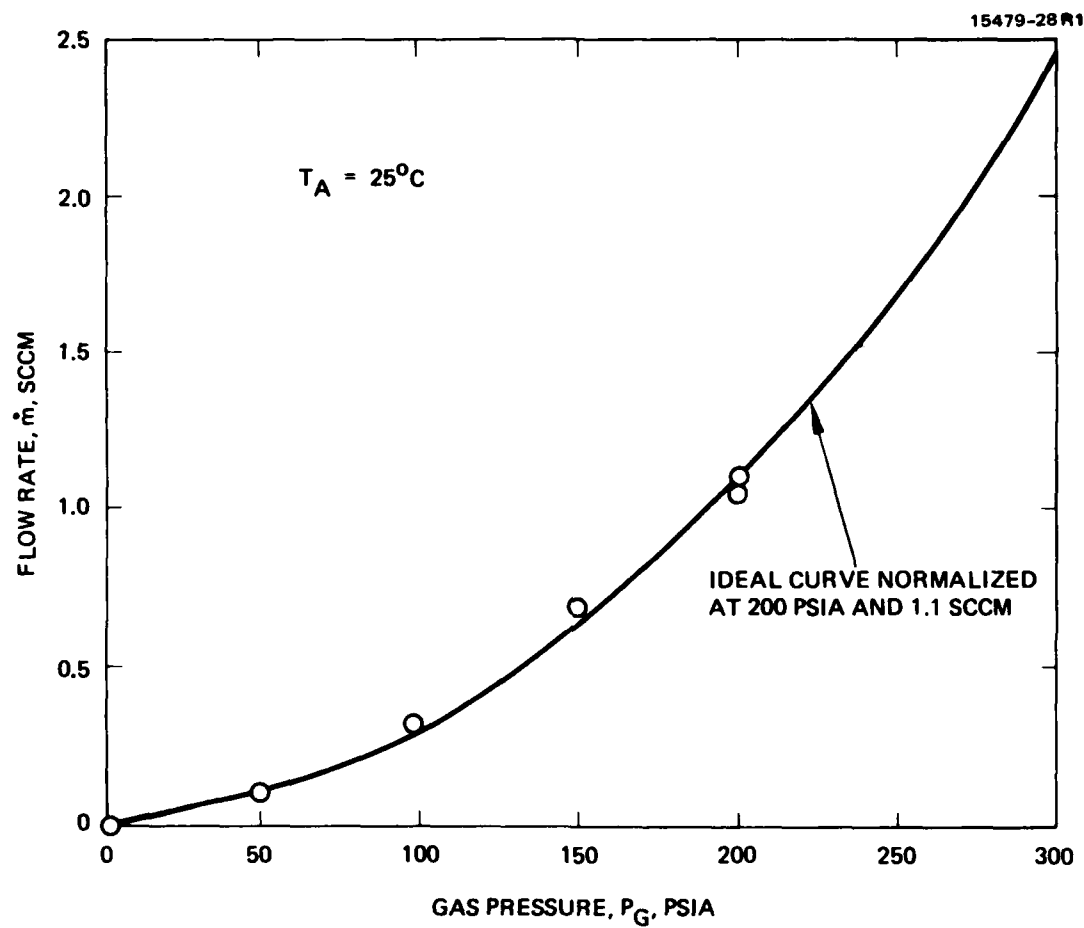


Figure 5-2. Flowrate versus gas pressure for the porous-tungsten flow impedance.

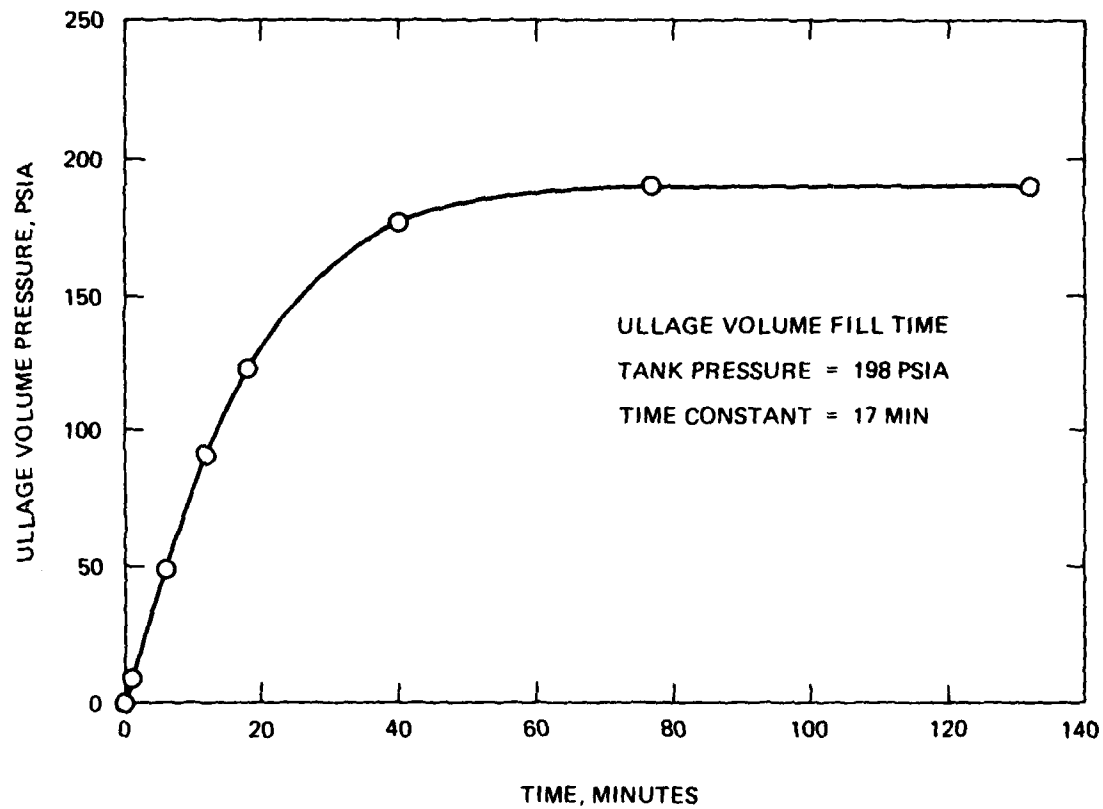


Figure 5-3. Time required to fill the ullage volume between the porous-tungsten plug and valve.

SECTION 6

SYSTEM TESTING

The PIES system is required to step through 16 logarithmically spaced current setpoints from 20 μA to 20 mA (a 1000:1 range) at three separate energy levels (0.5, 2.0, and 4.5 keV). The transfer function of the ion source (emission current out as a function of filament current input) varies drastically over this full dynamic range. We found it to be impossible to stabilize the emission current feedback loop over this dynamic range with a single gain setting in the electronics and still maintain acceptable response characteristics. Therefore, an analog multiplexer was added to the feedback loop so that the gain of the loop could be set to a separate value for each of the 16 current setpoints. The circuitry for multiplexing the gain is shown in Figure 4-8 (U1 and U2).

Figure 6-1 shows a typical sweep of the breadboard system through the 16 current setpoints and the 3 voltage setpoints. The response time between current setpoints (increasing current) is approximately 30 ms. This response is faster than the filament temperature response and is achieved because a change in filament voltage directly changes the discharge voltage of the ion source, which in turn directly changes the emission current. Therefore, the emission current rapidly responds to a change in filament voltage and then on a slower scale (~ 200 ms) to filament temperature.

The polarity of the filament voltage is critical to the correct response of the ion source to changes in current setpoint. If the filament voltage is positive, then an increase in filament voltage causes an increase in emission current and the feedback loop has negative feedback over the full frequency range. If, however, the filament voltage is negative, then an increase in filament voltage (more negative) will cause an

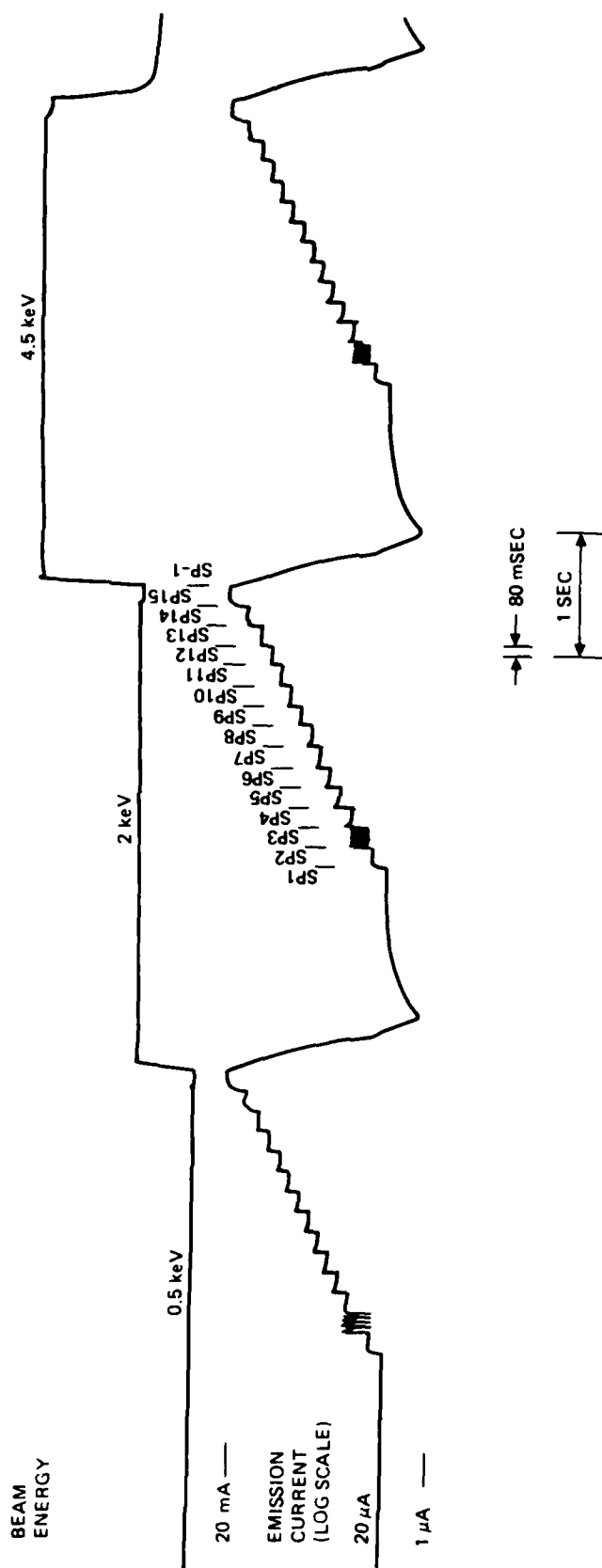


Figure 6-1. Strip chart recording of beam energy and emission current during a sweep of the breadboard PIES.

immediate decrease in emission current, followed by an increase in emission current as the filament temperature increases. To the feedback loop, this looks like positive feedback above ~ 50 Hz and negative feedback below ~ 50 Hz - clearly an undesirable situation.

The filament requires approximately 400 ms to cool down enough to decrease the emission current from 20 mA to 20 μ A in one step (Figure 6-1). The screen supply changes setpoints for increasing voltage in 50 ms and also in 100 ms for decreasing voltage, provided it is loaded to at least 20 mA. If the screen supply is unloaded, it requires several seconds to transition from 4.5 kV to 0.5 kV. Figure 6-1 also shows that current setpoint 3 (~ 50 μ A) is unstable. We were unable to find a cure for this instability by the time the breadboard system was delivered; however, this instability was eliminated in the flight system.

The stability problem with setpoint 3 was initially present in the flight system and, in fact, appeared to be slightly worse. Careful examination of the test data indicated that the plasma inside the discharge chamber of the ion source was mode-shifting at this point and therefore a stable operating point did not exist. As described in the paragraph which follows, the configuration of the power supply connections to the source was changed to produce a parallel discharge path (a quasi-keeper electrode) in the source that generates a substantial amount of plasma, even when the emission current from the source is less than 1 μ A. This increase in plasma density shifts the operating conditions in the discharge chamber to a point where the mode-shift has already occurred for the full range of operation of the source.

The system configuration used for breadboard testing and early testing of the flight system is shown in Figure 6-2. In this configuration (in which the discharge instability was present) the negative side of the discharge supply is connected to the discharge chamber of the source and plasma is generated

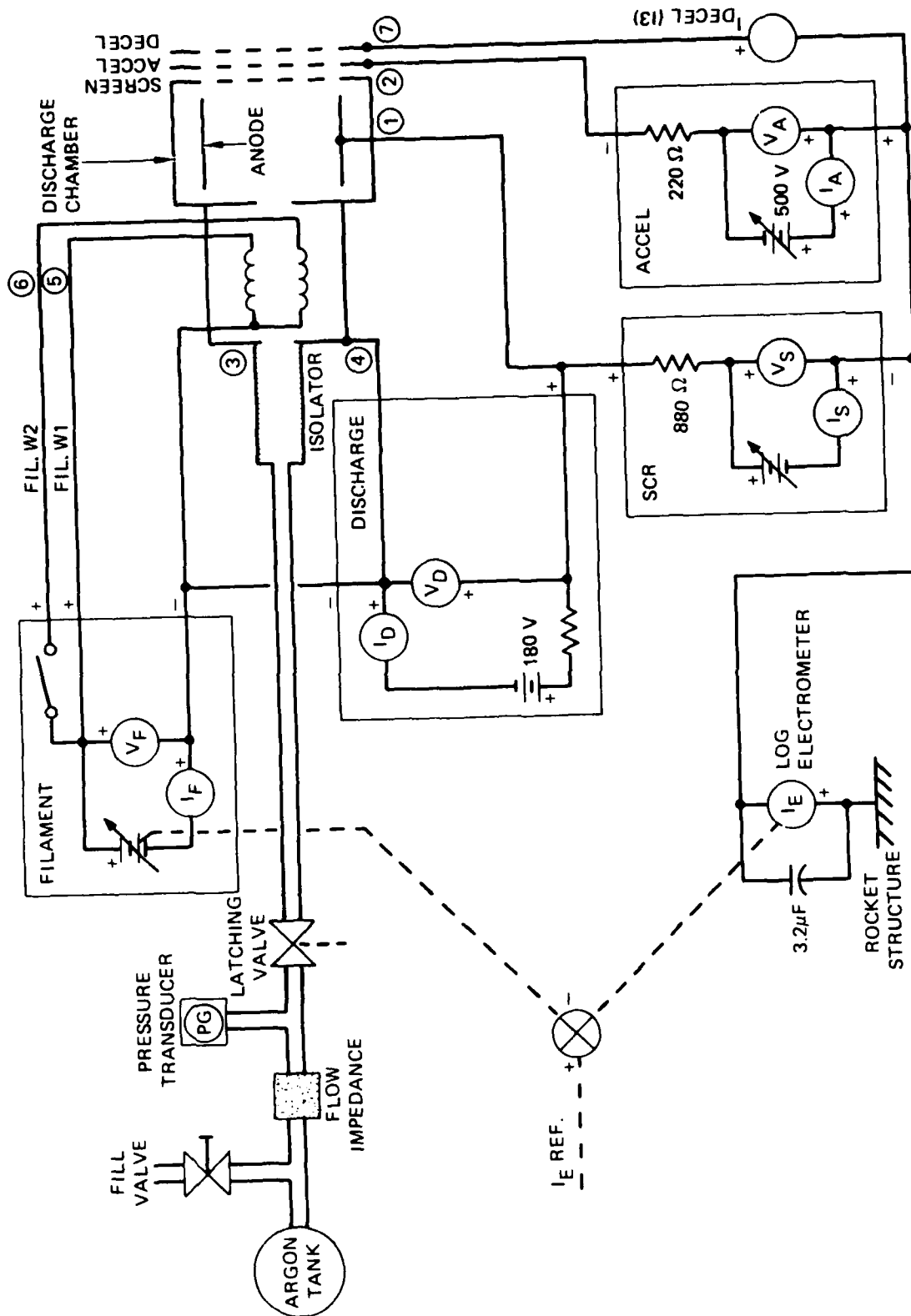
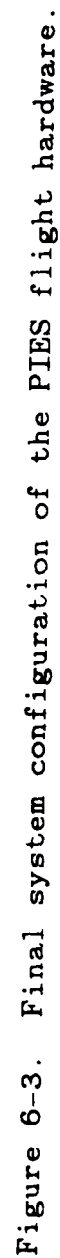


Figure 6-2. System configuration for the breadboard and early testing of the flight hardware.

between the anode and the filament. Figure 6-3 shows the final configuration of the flight system (in which the discharge instability was eliminated) where the negative side of the discharge supply is connected to the negative side of the filament supply and the discharge chamber (including the screen grid) is connected to the positive side of the discharge supply through a 2200- Ω resistor and 0.56- μ F capacitor. In this configuration plasma is generated between the discharge chamber and the filament as well as between the anode and the filament. The plasma between the anode and the filament still controls the emission current from the source, while the plasma between the discharge chamber and the filament increases the plasma density in the vicinity of the filament in order to avoid the mode-shift.

The emission-current feedback loop was also modified during testing of the flight system. The early configuration is shown in Figure 6-4. The loop is compensated by an integrator and a lead network; the Bode plots for it are shown in Figure 6-5. The integrator in this loop was causing overshoot and long settling times during step changes in emission current. The feedback loop was changed to the configuration shown in Figure 6-6, where the integrator is now inside of a minor loop. The integrator still removes the nonlinearities and variations with input voltage of the filament supply, but does not appear in the transfer function of the major loop. The Bode plots for this loop are shown in Figure 6-7 and show larger gain and phase margins than the earlier configuration (Figure 6-5).

The response characteristics of the flight system as it steps through the 16 current setpoints and the 3 energy levels are presented in Figure 6-8. The emission current settles within 20 ms with no overshoot for all steps except for the step from 1 μ A to 20 μ A which has a slight overshoot and a settling time of 40 ms. Figure 6-8 also shows the screen voltage, filament current, discharge voltage, discharge current, 15-V housekeeping voltage, and command strobe as the emission current is being stepped.



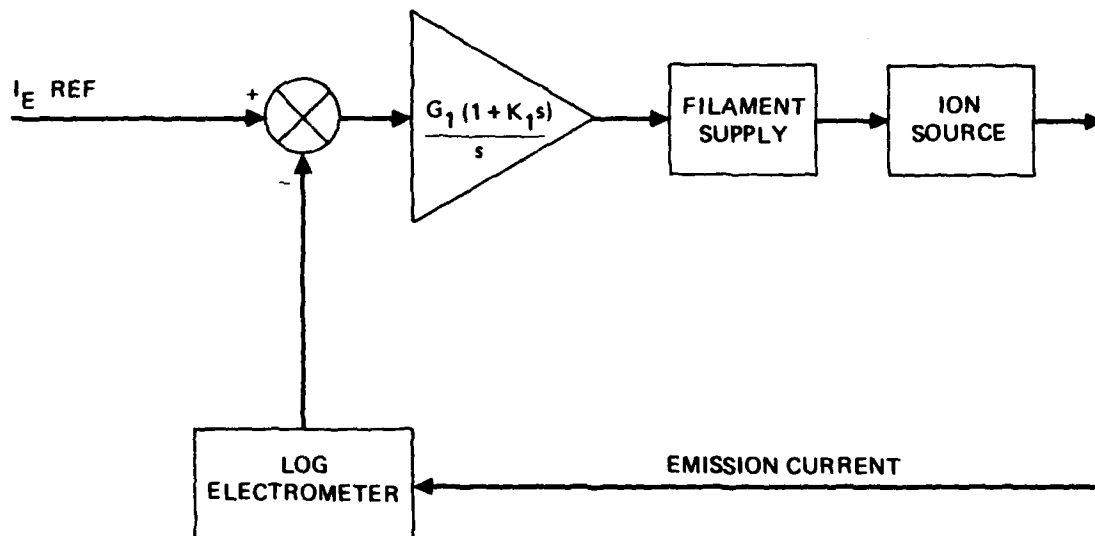


Figure 6-4. Emission-current feedback loop of the bread-board and during early testing of the flight hardware.

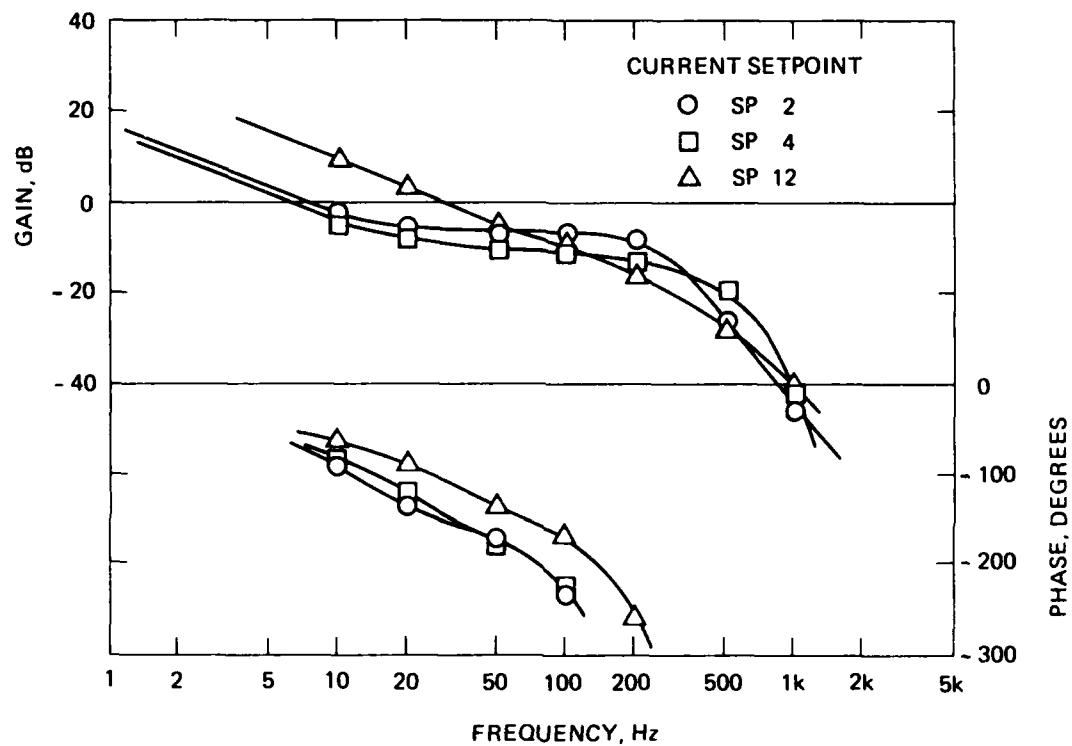


Figure 6-5. Bode plots of the emission-current feedback loop for the breadboard and early testing of the flight hardware.

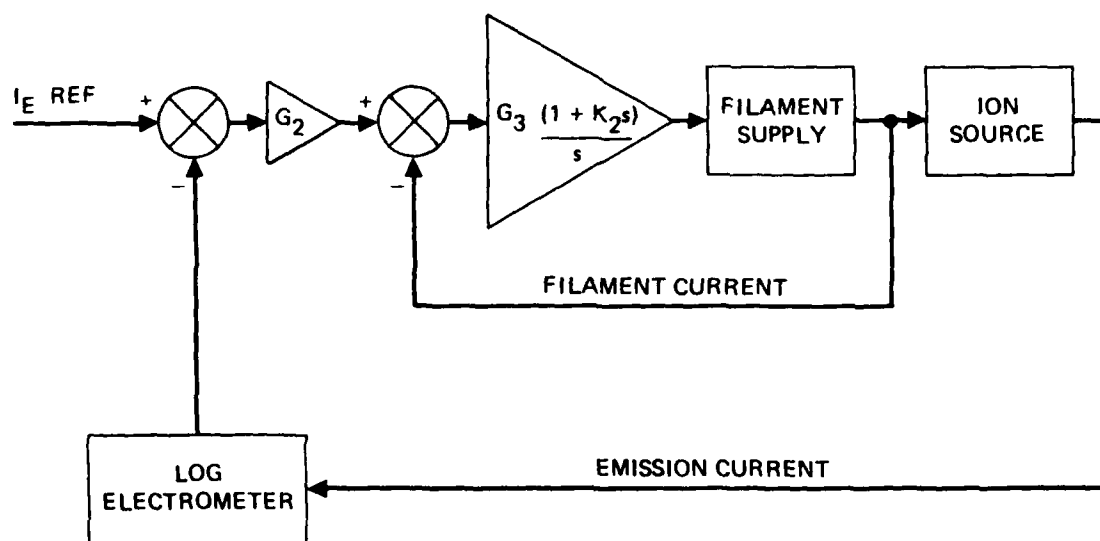


Figure 6-6. Final emission-current feedback loop.

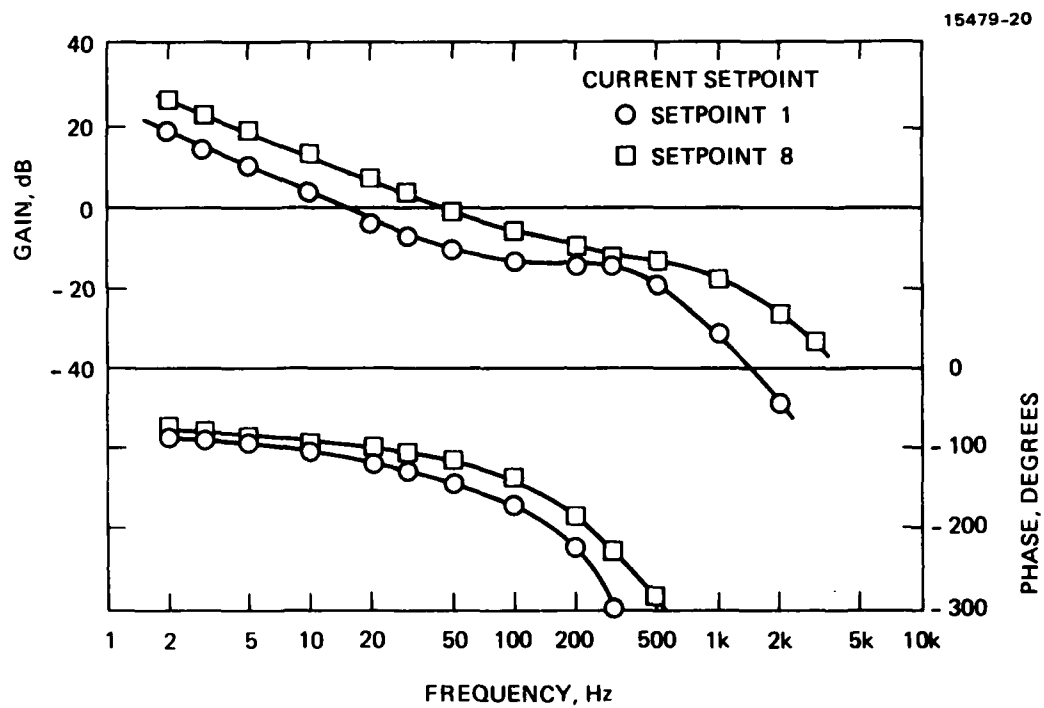


Figure 6-7. Bode plots for the final emission-current feedback loop.

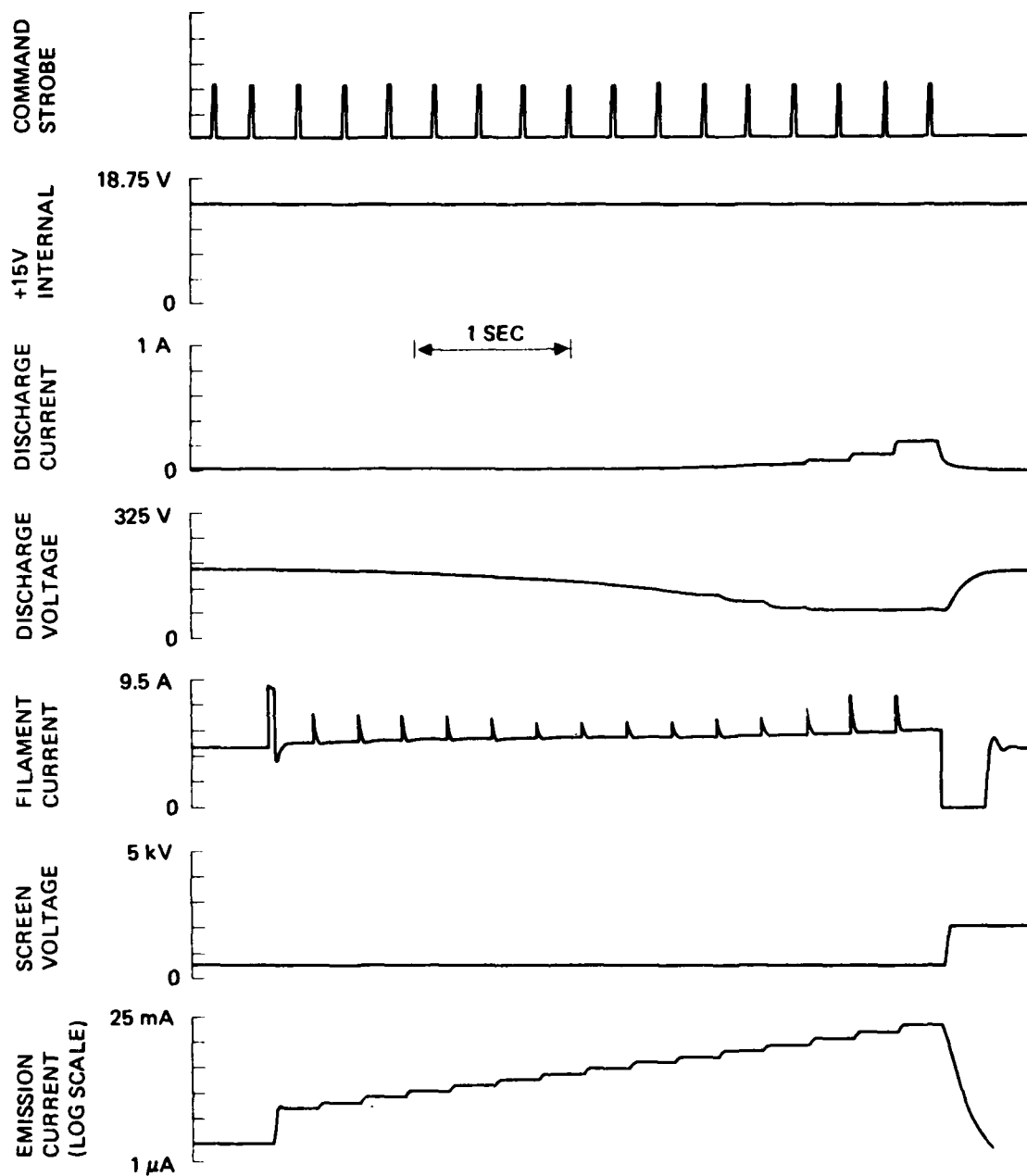


Figure 6-8(a). Response of the flight system as it steps through its current setpoints at a beam energy of 500 V.

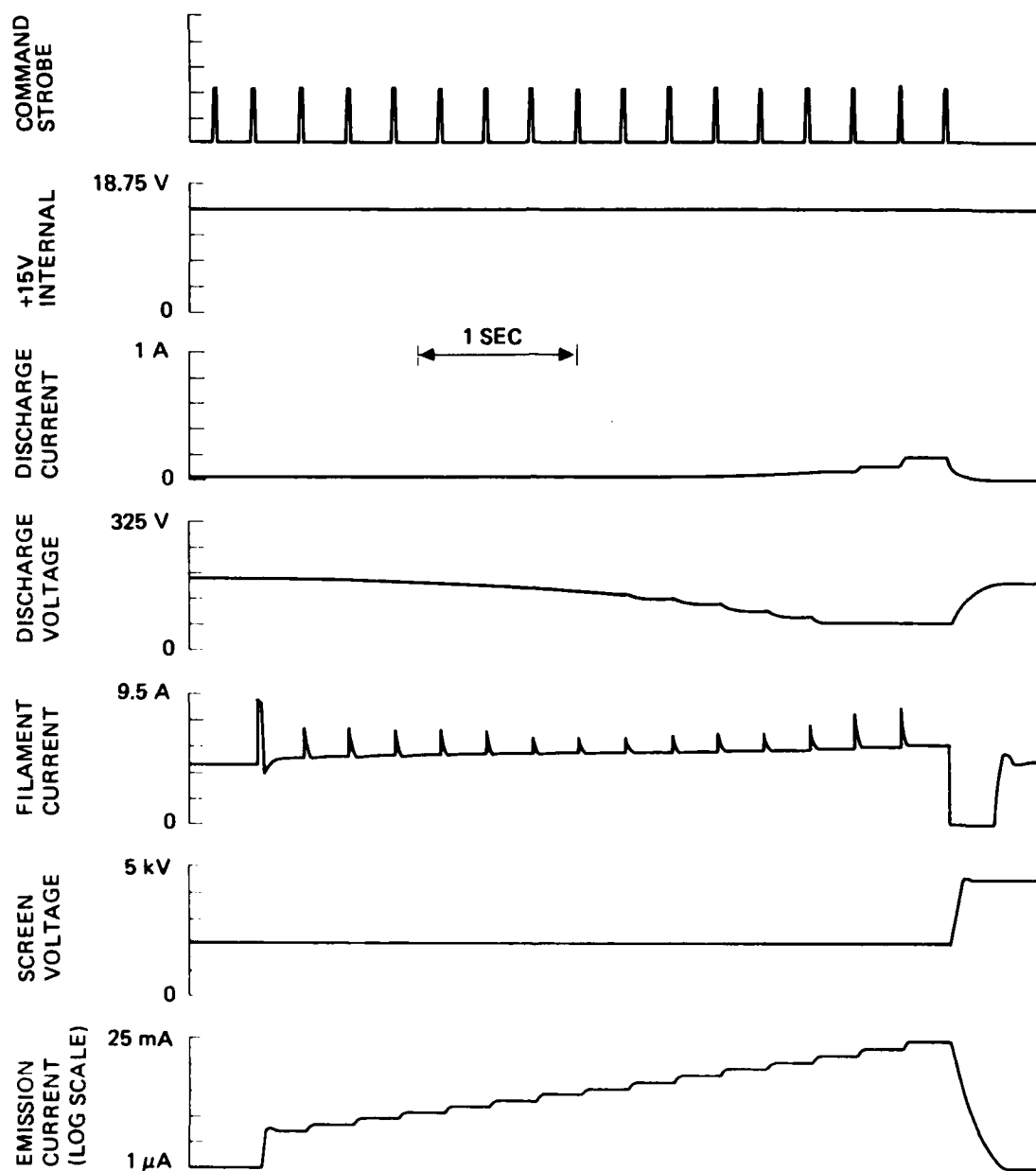


Figure 6-8(b). Response of the flight system as it steps through its 16 current setpoints at a beam energy of 2 kV.

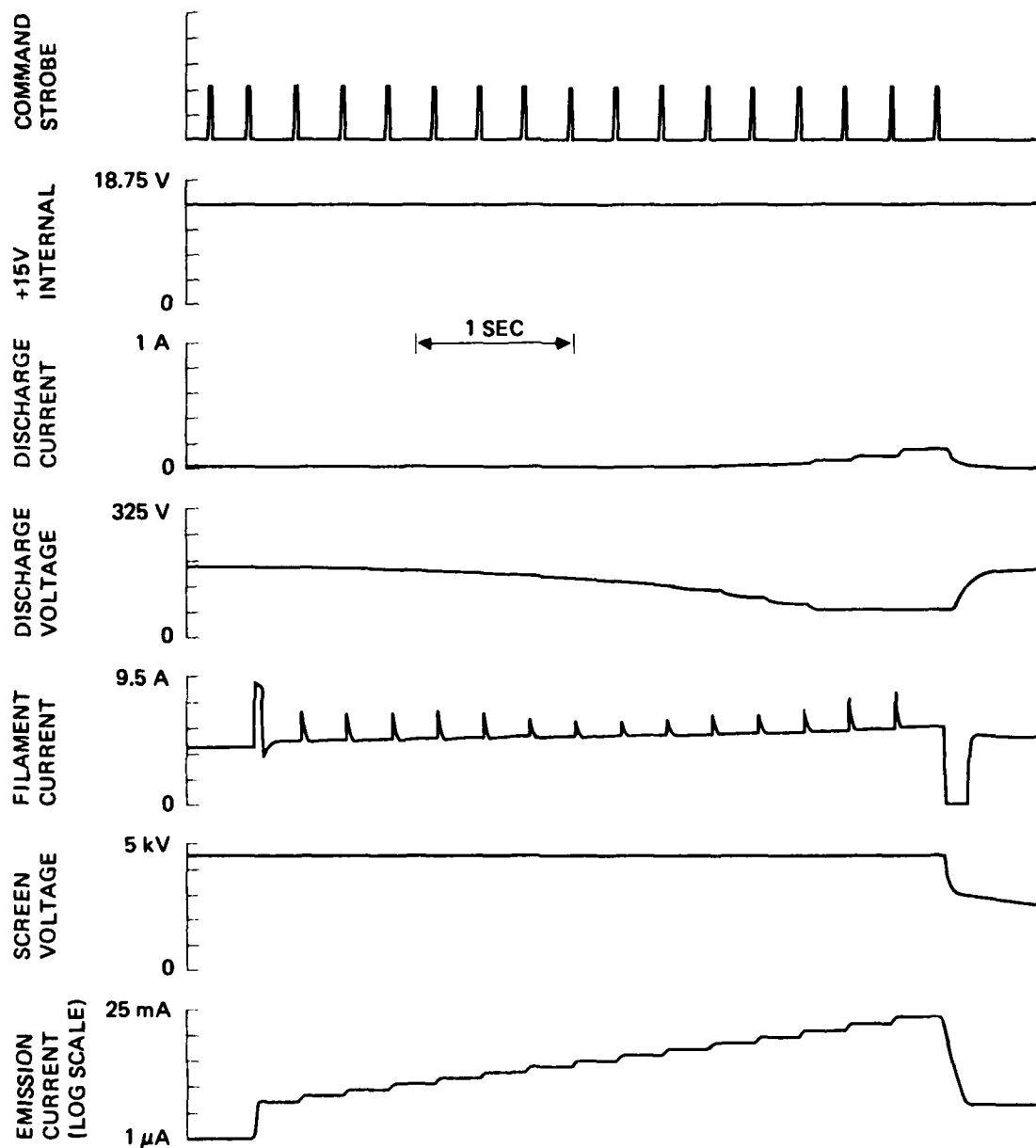


Figure 6-8(c). Response of the flight system as it steps through its 16 current setpoints at a beam energy of 4.5 kV.

The operating parameters of the flight system for all 16 current setpoints at each of the 3 beam-energy levels are presented in Table 6-1. The values measured with external meters, the telemetry voltage readings, and the GSE (ground support equipment) readings are all listed in the Table. Figure 6-9 shows the input power required by the flight system for all of its operating points. The telemetry calibration curves are presented in Figures 6-10 through 6-21.

Table 6-1(b). Operating Parameters of the Flight System for a Beam Energy of 2 kV

15479-15

SE POINT	V _S	I _E				I _S				V _S				I _D				V _D					
		I _E mA	I _E TLM V	GSE mA	I _E TLM V	I _S mA	I _S TLM V	GSE A	V _S V	V _S TLM V	GSE V	I _S mA	I _S TLM V	GSE A	I _D mA	I _D TLM V	GSE A	V _D V	V _D TLM V	GSE V			
0	M	0.001	-0.01	0.0011	0.003	0.28	0.08	0	2020	2.04	2057	0.003	0.28	0	0.13	0	0	185.0	3.39	171.7			
1	M	0.020	1.40	0.0192	0.113	4.37	0.08	0	2020	2.04	2057	0.113	4.37	0.0044	0.15	0.0044	10.1	182.4	3.39	171.7			
2	M	0.034	1.65	0.0322	0.209	6.55	0.08	0	2020	2.04	2057	0.209	6.55	0.0069	0.16	0.0069	15.1	181.0	3.39	171.7			
3	M	0.055	1.85	0.0539	0.371	9.09	0.09	0	2020	2.04	2057	0.371	9.09	0.0133	0.17	0.0133	20.9	178.5	3.39	171.7			
4	M	0.089	2.12	0.0835	0.629	11.52	0.10	0	2020	2.04	2057	0.629	11.52	0.019	0.18	0.0133	26.5	178.2	3.39	171.7			
5	M	0.146	2.36	0.140	1.03	13.82	0.11	0	2020	2.04	2057	1.03	13.82	0.020	0.20	0.0177	31.8	176.8	3.39	171.7			
6	M	0.240	2.60	0.225	1.59	15.65	0.13	0.0001597	2020	2.03	2057	1.59	15.65	0.021	0.21	0.0177	36.1	175.7	3.39	171.7			
7	M	0.392	2.84	0.363	2.49	16.94	0.16	0.0003194	2020	2.04	2057	2.49	16.94	0.022	0.22	0.0221	39.2	174.7	3.39	171.7			
8	M	0.647	3.08	0.585	4.17	18.43	0.19	0.0007965	2020	2.04	2057	4.17	18.43	0.023	0.23	0.0221	42.8	173.4	3.39	171.7			
9	M	1.07	3.32	0.980	7.70	19.93	0.25	0.0012776	2020	2.04	2057	7.70	19.93	0.025	0.25	0.0310	46.7	171.3	3.39	171.7			
A	M	1.75	3.56	1.64	12.8	22.70	0.33	0.0019164	2020	2.03	2057	12.8	22.7	0.027	0.27	0.0354	52.8	162.8	3.26	165.2			
B	M	2.90	3.81	2.75	20.0	28.80	0.48	0.0031940	2020	2.04	2057	20.0	28.8	0.032	0.32	0.0443	65.7	138.4	2.86	142.6			
C	M	4.53	4.04	4.26	31.1	33.30	0.71	0.0046928	2020	2.04	2057	31.1	33.3	0.037	0.37	0.0531	80.4	112.7	2.36	114.5			
D	M	7.66	4.31	7.43	55.3	28.90	1.19	0.0076978	2010	2.03	2057	55.3	28.9	0.044	0.44	0.0708	74.0	88.1	1.86	87.5			
E	M	12.51	4.57	13.0	98.8	25.50	2.04	0.0135290	2000	2.03	2057	98.8	25.5	0.059	0.59	0.1062	59.5	66.9	1.44	63.7			
F	M	20.2	4.85	22.6	177	25.20	3.45	0.0205444	2000	2.03	2038	177	25.2	0.93	0.93	0.1959	58.1	64.5	1.44	63.7			
SE POINT		INPUT POWER																			P _T		
		I _A mA	I _A TLM V	GSE A	V _A V	V _A TLM V	GSE V	I _E A	I _E TLM V	GSE A	V _E V	V _E TLM V	GSE V	I _S mA	I _S TLM V	GSE A	V _S V	I _D mA	I _D TLM V	GSE A	V _D V	V _D TLM V	GSE V
0		0.037	1.70	0	-535	4.11	534	4.29	2.24	4.22	3.95	1.20	4.0	0.064	0.06	0	2.82	27.9	73.1	4.11	4.07	-0.11	
1		0.039	1.76	0	-535	4.11	534	4.76	2.49	4.66	4.73	1.38	4.8	0.064	0.06	0	2.86	27.9	82.6				
2		0.040	1.76	0	-535	4.11	534	4.84	2.53	4.73	4.87	1.41	4.9	0.066	0.06	0	3.04	27.9	84.8				
3		0.041	1.77	0	-535	4.11	534	4.91	2.56	4.80	4.99	1.44	5.0	0.067	0.06	0	3.12	27.9	87.0	4.11	4.07	-0.11	
4		0.042	1.78	0	-535	4.11	534	4.96	2.59	4.84	5.08	1.46	5.1	0.069	0.06	0	3.18	27.9	88.7				
5		0.044	1.79	0	-535	4.11	534	5.00	2.61	4.88	5.16	1.48	5.2	0.072	0.07	0	3.24	27.9	90.4				
6		0.045	1.79	0.00002	-535	4.11	534	5.03	2.62	4.91	5.21	1.49	5.2	0.075	0.07	0	3.28	27.9	91.8				
7		0.046	1.80	0.00002	-535	4.11	534	5.04	2.63	4.91	5.24	1.49	5.2	0.079	0.07	0	3.36	27.9	93.7				
8		0.047	1.80	0.00002	-535	4.11	534	5.06	2.64	4.95	5.27	1.50	5.2	0.085	0.08	0	3.46	27.9	96.5	4.11/5.22	4.07/5.4	-0.11/0	
9		0.048	1.81	0.00002	-534	4.11	534	5.07	2.65	4.98	5.30	1.51	5.3	0.082	0.08	0	3.56	27.9	98.3				
A		0.050	1.81	0.00002	-534	4.11	534	5.07	2.65	4.98	5.31	1.51	5.3	0.083	0.08	0	3.64	27.9	101.6				
B		0.064	1.82	0.00006	-534	4.11	534	5.12	2.67	5.02	5.40	1.53	5.4	0.077	0.07	0	3.75	27.9	104.6				
C		0.061	1.83	0.00006	-534	4.11	534	5.19	2.71	5.09	5.55	1.56	5.6	0.067	0.06	0	3.89	27.8	108.1				
D		0.075	1.82	0.00006	-533	4.10	534	5.27	2.75	5.17	5.70	1.60	5.6	0.087	0.08	0	4.15	27.8	115.4				
E		0.087	1.87	0.00012	-533	4.10	534	5.39	2.82	5.27	5.86	1.66	5.9	0.071	0.07	0	4.59	27.8	127.6				
F		0.131	1.93	0.00017	-532	4.10	531	5.58	2.91	5.46	6.34	1.74	6.3	0.065	0.06	0	5.51	27.8	133.2	4.11	4.06	-0.11	

Table 6-1(c). Operating Parameters of the Flight System for a Beam Energy of 4.5 kV

15479-14

IE SETPOINT	IS				VS				ID				VD			
	IS mA	IS TLMV	IS GSE	IS mA	VS V	VS TLMV	VS GSE	VS V	ID mA	ID TLMV	ID GSE	ID V	VD V	VD TLMV	VD GSE	VD V
0	0.001	-0.01	0.0017	0.016	4530	4.57	4581	4530	0.016	0.13	0	1.4	185.1	1.38	171.7	185.1
1	0.020	1.41	0.0200	0.208	4510	4.57	4581	4510	0.208	0.15	0.0044	7.7	183.3	3.39	171.7	183.3
2	0.034	1.66	0.0335	0.330	4500	4.56	4581	4500	0.330	0.16	0.0044	10.9	182.4	3.39	171.7	182.4
3	0.065	1.89	0.0639	0.519	4500	4.56	4581	4500	0.519	0.17	0.0088	14.8	181.3	3.39	171.7	181.3
4	0.089	2.12	0.0869	0.783	4490	4.56	4581	4490	0.783	0.18	0.0133	19.9	180.0	3.39	171.7	180.0
5	0.148	2.36	0.146	1.257	4490	4.56	4581	4490	1.257	0.19	0.0177	26.1	178.3	3.39	172.8	178.3
6	0.241	2.60	0.225	1.991	4490	4.56	4581	4490	1.991	0.21	0.0177	31.4	176.9	3.39	171.7	176.9
7	0.366	2.84	0.378	2.85	4490	4.56	4581	4490	2.85	0.22	0.0221	35.0	175.8	3.39	172.8	175.8
8	0.551	3.08	0.608	4.42	4480	4.56	4581	4480	4.42	0.23	0.0221	38.2	174.6	3.39	171.7	174.6
9	1.08	3.32	1.02	7.57	4480	4.56	4581	4480	7.57	0.25	0.0310	42.1	172.7	3.39	171.7	172.7
A	1.76	3.56	1.71	12.96	4480	4.55	4581	4480	12.96	0.28	0.0354	46.9	168.9	3.38	171.7	168.9
B	2.91	3.81	2.75	21.0	4480	4.56	4581	4480	21.0	0.32	0.0487	56.7	151.5	3.07	154.4	151.5
C	4.54	4.04	4.43	30.4	4480	4.55	4581	4480	30.4	0.37	0.0576	69.2	126.2	2.61	128.5	126.2
D	7.68	4.31	7.73	51.6	4470	4.55	4581	4470	51.6	0.45	0.0753	76.7	95.8	2.03	97.2	95.8
E	12.54	4.57	13.5	90.9	4470	4.56	4581	4470	90.9	0.56	0.1018	61.0	68.4	1.48	66.9	68.4
F	20.4	4.85	23.5	156.4	4460	4.56	4581	4460	156.4	0.80	0.1594	58.4	65.4	1.45	63.7	65.4
IE SETPOINT	VA				VF				IDCELL				INPUT POWER			
	VA mA	VA TLMV	VA GSE	VA V	VF V	VF TLMV	VF GSE	VF V	IDCELL mA	IDCELL TLMV	IDCELL GSE	IDCELL V	INPUT POWER V IN	INPUT POWER V IN	INPUT POWER V IN	INPUT POWER V IN
0	0.109	1.78	0	-533	4.11	534	4.75	4.19	0.335	0.33	0.00030	2.99	27.9	83.4	4.11	4.08
1	0.134	1.85	0.00007	-533	4.11	534	4.71	4.58	0.361	0.35	0.00034	3.36	27.9	93.7		
2	0.146	1.86	0.00009	-533	4.11	534	4.78	4.69	0.387	0.35	0.00036	3.45	27.9	98.3		
3	0.161	1.90	0.00014	-533	4.11	531	4.84	4.73	0.381	0.37	0.00036	3.53	27.9	98.5	4.11	4.07
4	0.176	1.92	0.00017	-532	4.10	531	4.90	4.86	0.385	0.38	0.00038	3.62	27.9	101.0		
5	0.193	1.94	0.00019	-532	4.10	531	4.96	4.94	0.409	0.41	0.00041	3.73	27.9	104.1		
6	0.211	1.96	0.00021	-531	4.10	531	5.00	4.88	0.426	0.42	0.00040	3.82	27.9	106.6		
7	0.225	1.98	0.00024	-531	4.10	531	5.02	4.91	0.453	0.44	0.00041	3.92	27.9	109.4		
8	0.263	2.00	0.00026	-531	4.10	531	5.04	4.91	0.531	0.50	0.00049	4.03	27.8	112.0	4.11	4.07
9	0.280	2.03	0.00031	-531	4.10	531	5.07	4.96	0.558	0.49	0.00053	4.20	27.8	116.8		
A	0.304	2.05	0.00033	-531	4.10	531	5.08	4.98	0.550	0.55	0.00053	4.44	27.8	123.4		
B	0.323	2.08	0.00038	-531	4.10	531	5.12	5.02	0.596	0.59	0.00058	4.70	27.8	130.7		
C	0.430	2.12	0.00040	-531	4.09	531	5.19	5.06	0.636	0.62	0.00056	5.07	27.8	140.9		
D max	0.600	2.31	0.00066	-530	4.09	531	5.28	5.17	0.629	0.62	0.00062	5.77	27.8	160.4		
E	0.306	2.15	0.00043	-529	4.09	531	5.38	5.27	0.810	0.82	0.00079	6.87	27.7	190.3		
F	0.358	2.22	0.00052	-528	4.08	529	5.53	5.42	0.860	0.86	0.00088	8.80	27.6	242.9	4.11	4.08

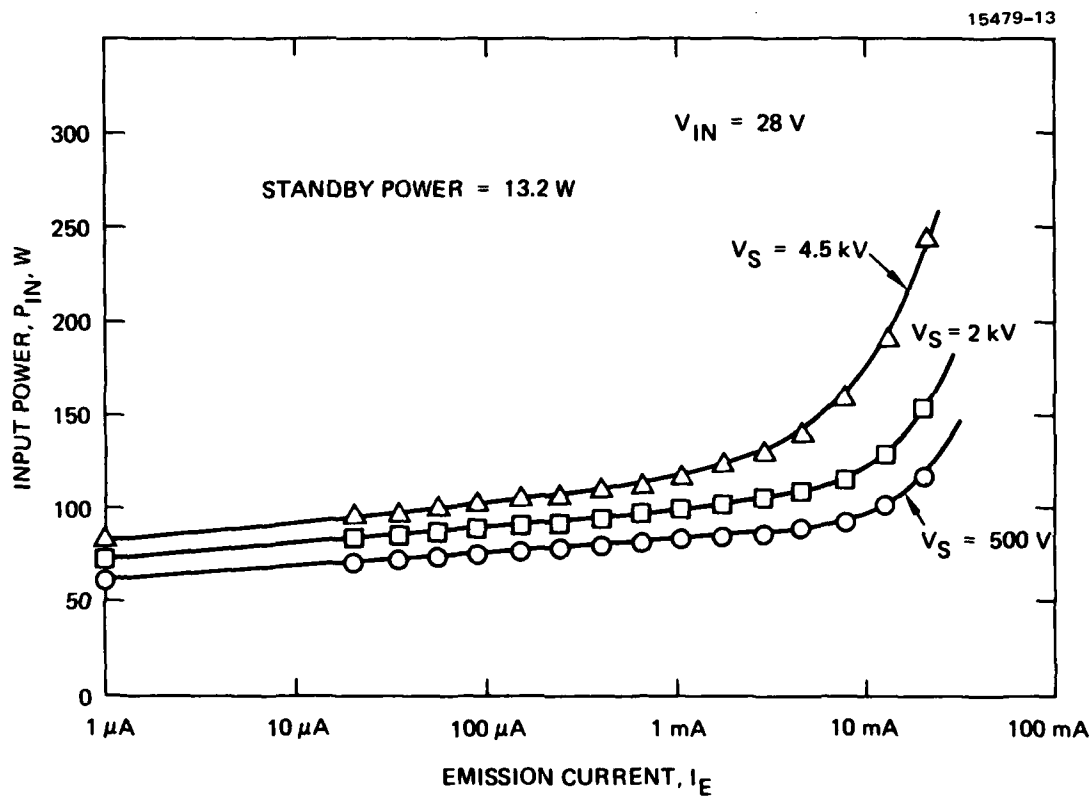


Figure 6-9 Input power required by the flight system for all operating points.

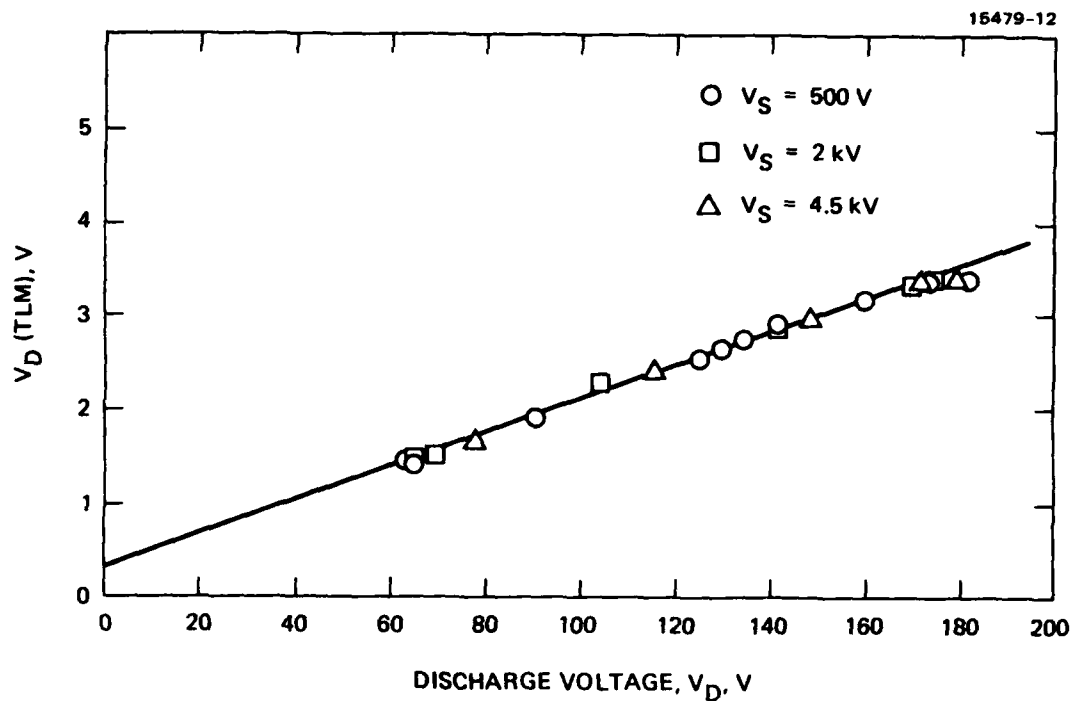


Figure 6-10. Telemetry calibration curve for the discharge voltage.

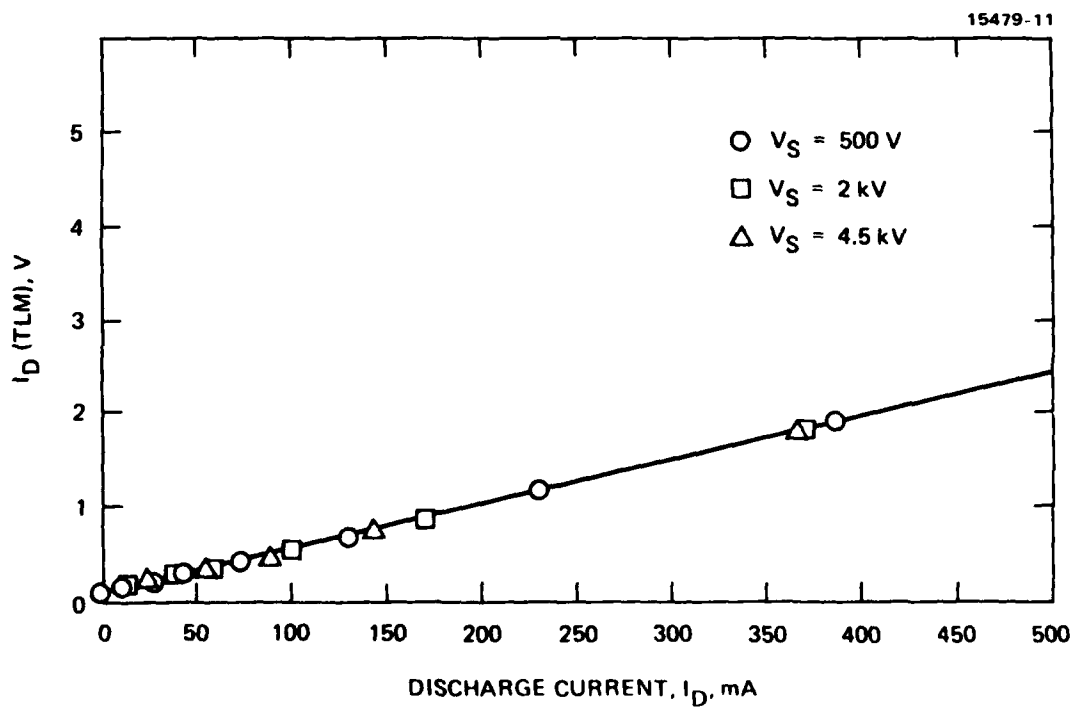


Figure 6-11. Telemetry calibration curve for the discharge current.

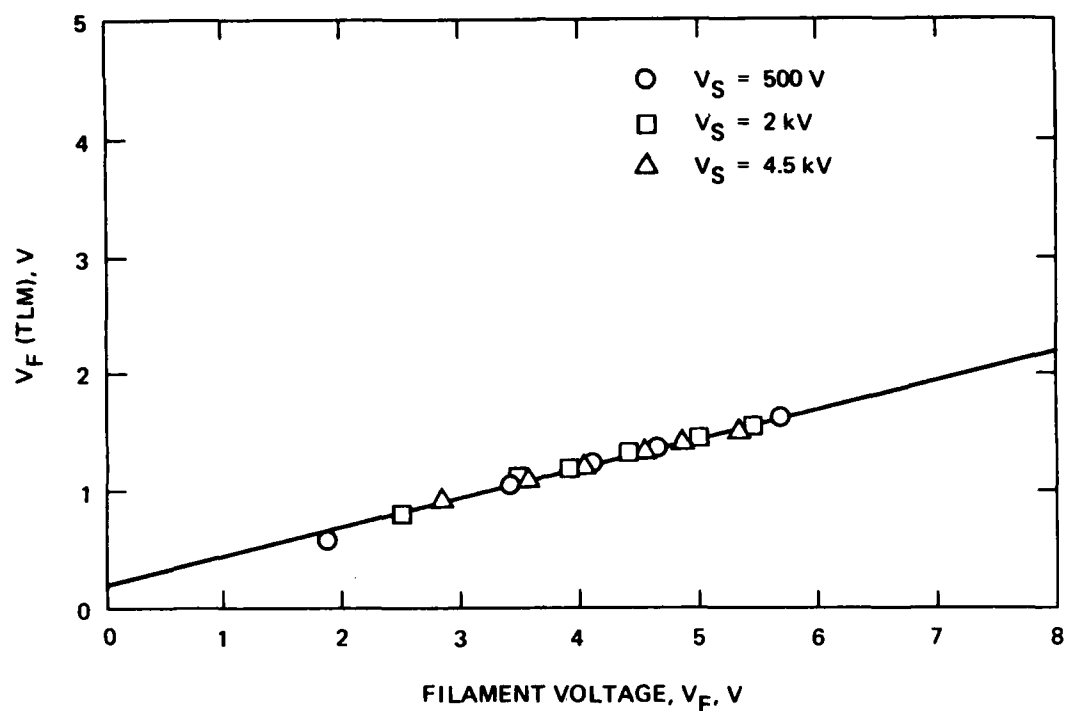


Figure 6-12. Telemetry calibration curve for the filament voltage.

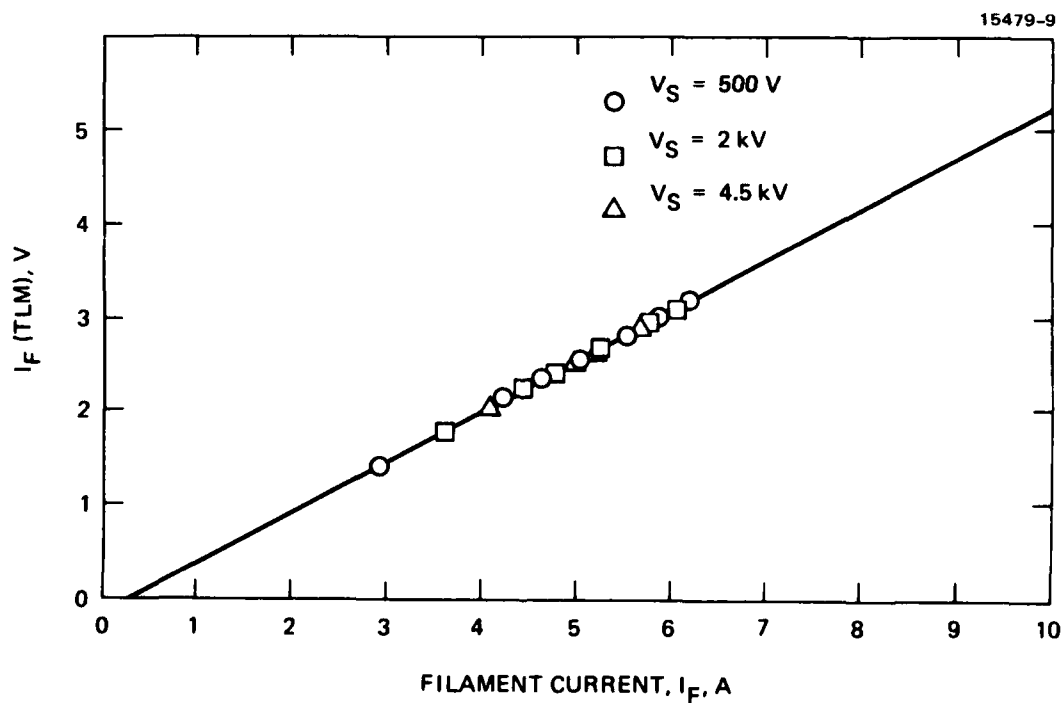


Figure 6-13. Telemetry calibration curve for the filament current.

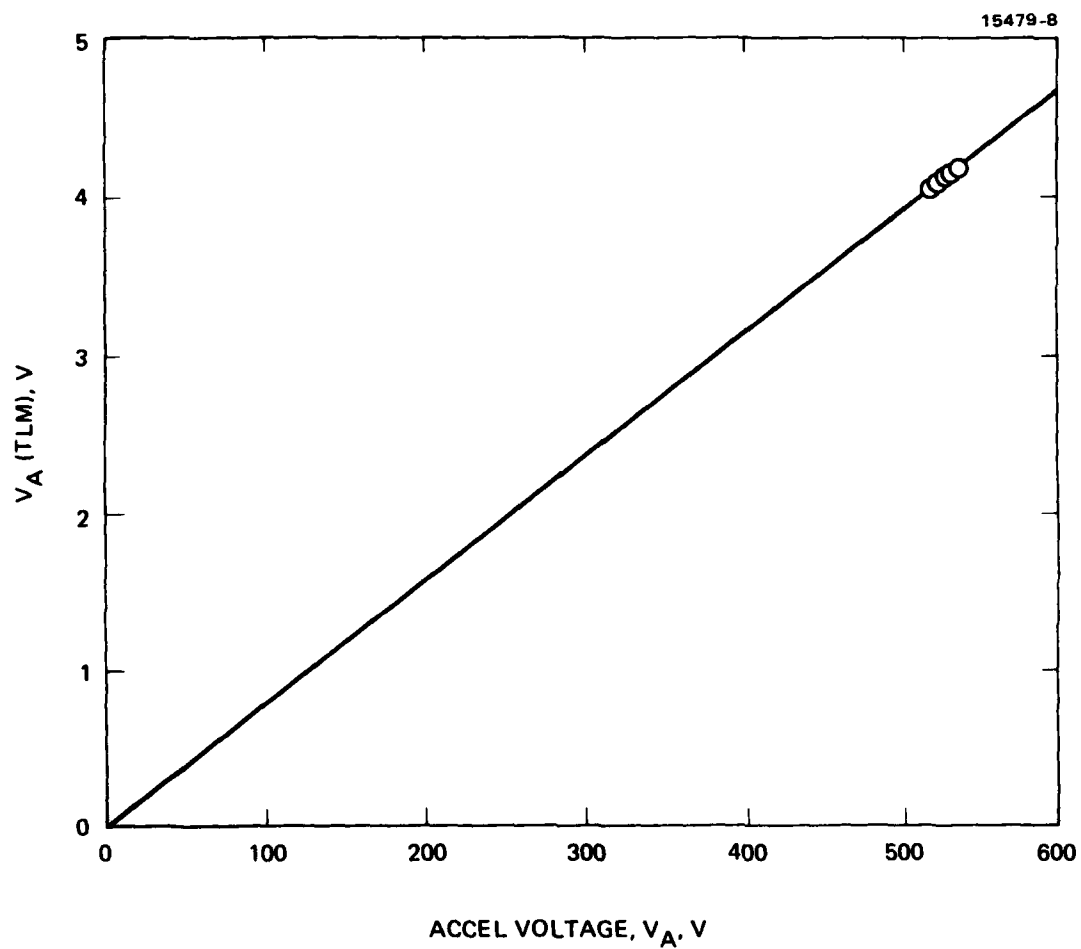


Figure 6-14. Telemetry calibration curve for the accel voltage.

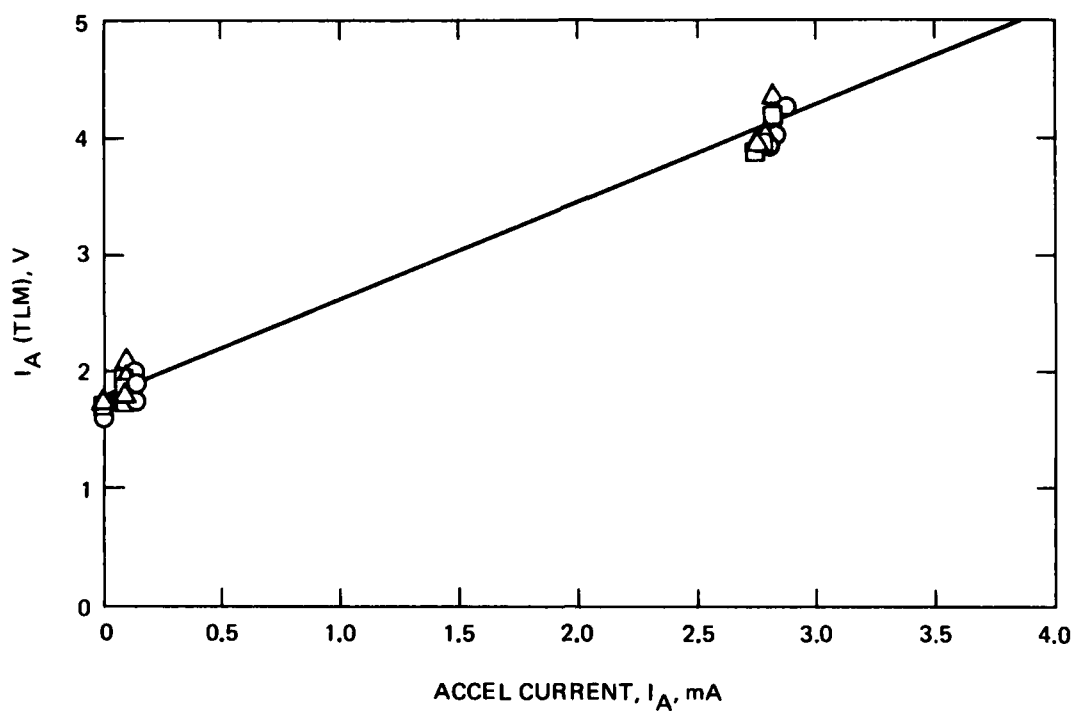


Figure 6-15. Telemetry calibration curve for the accel current.

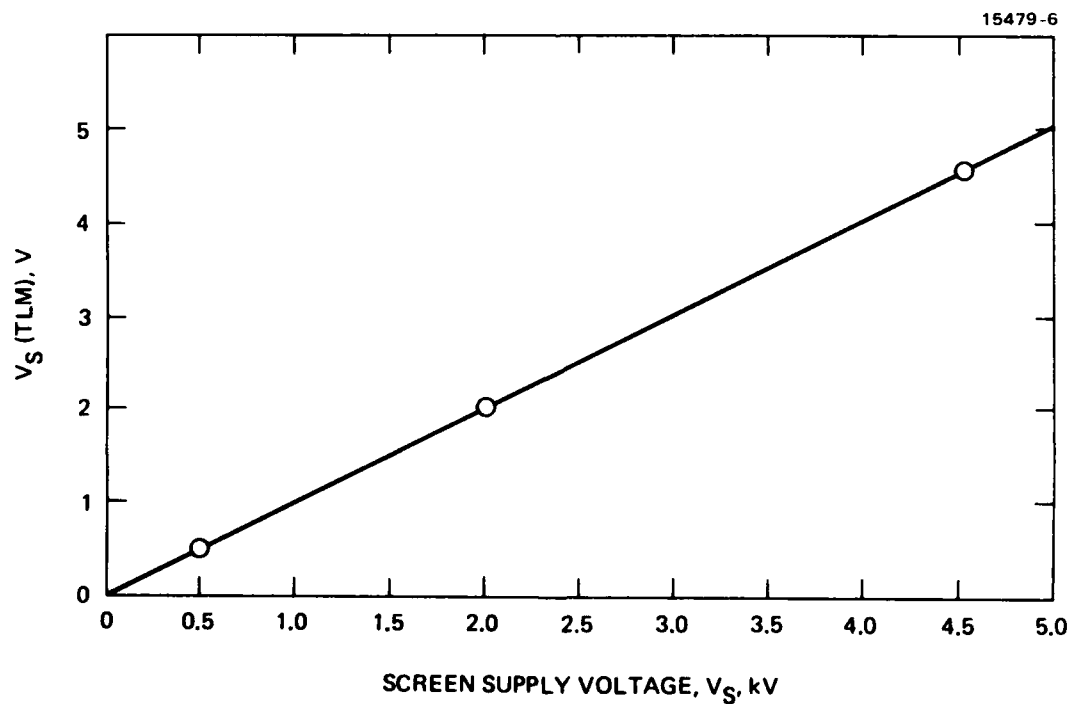


Figure 6-16. Telemetry calibration curve for the screen voltage.

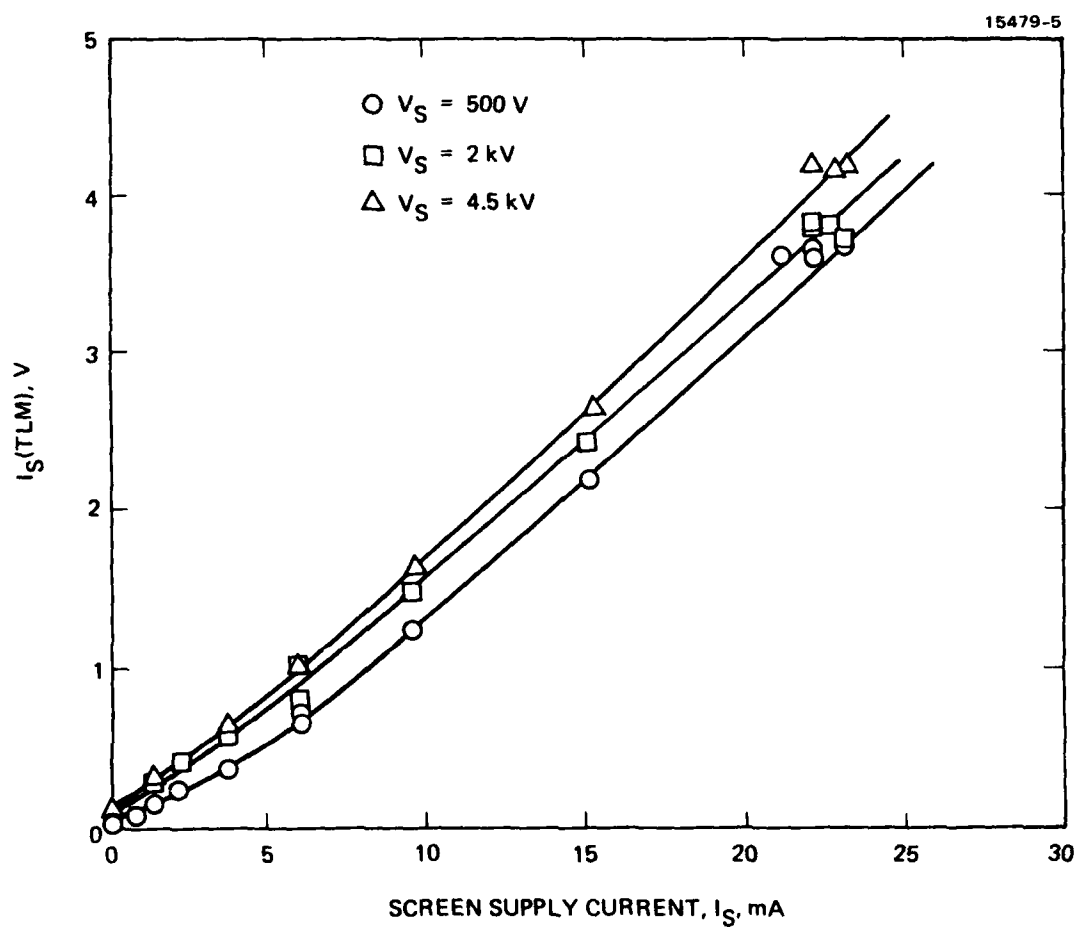


Figure 6-17. Telemetry calibration curve for the screen current.

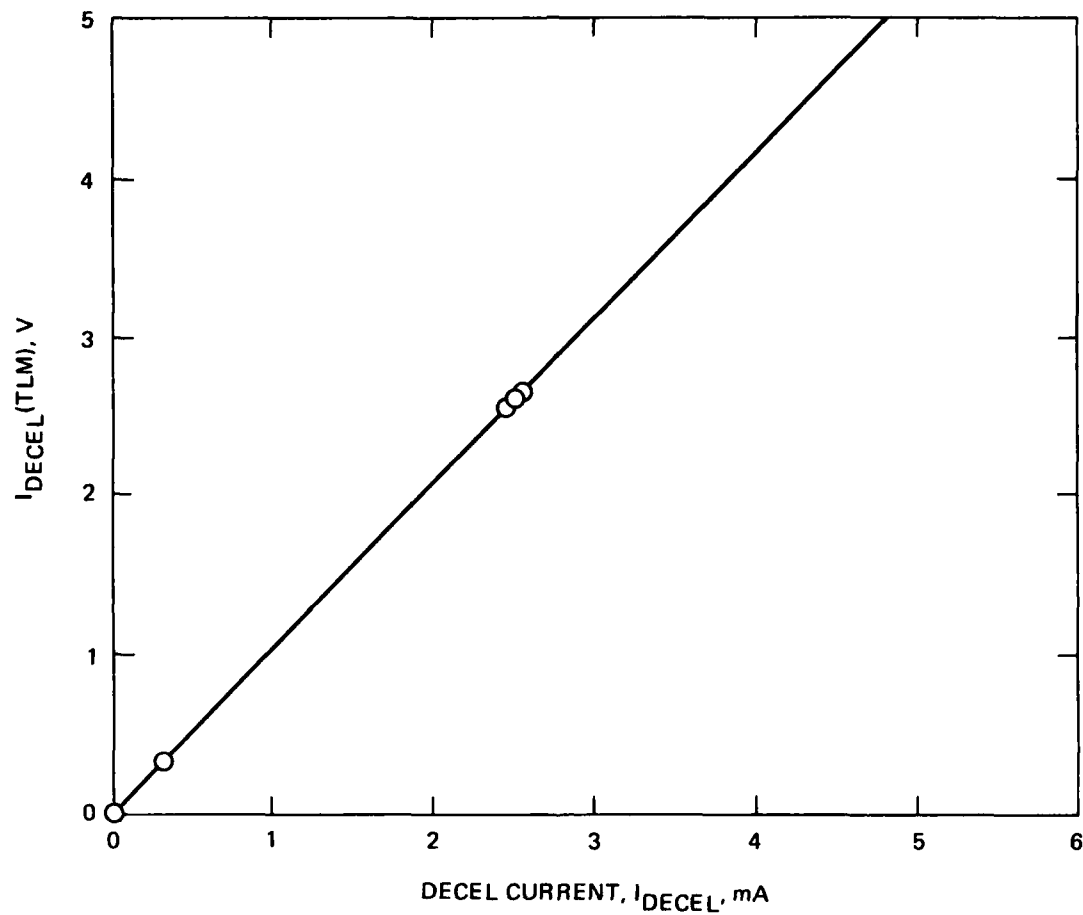


Figure 6-18. Telemetry calibration curve for the decel current.

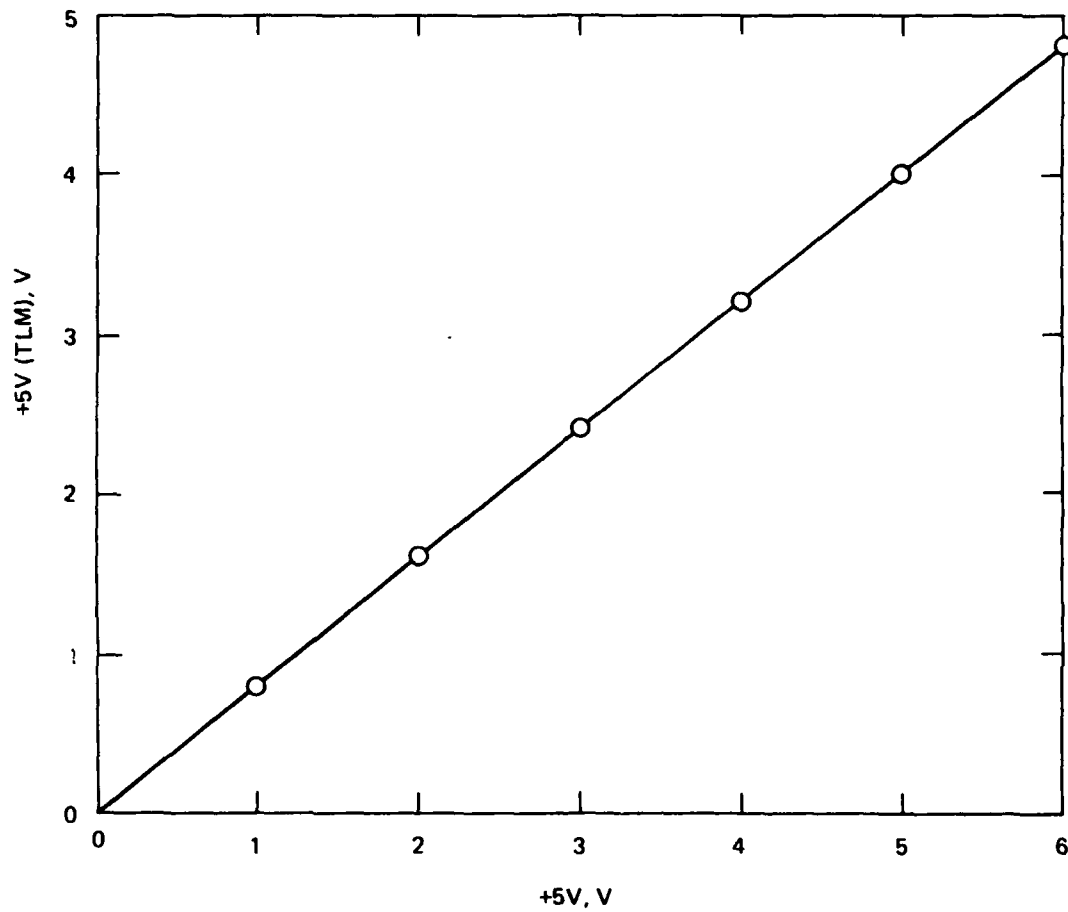


Figure 6-19. Telemetry calibration curve for the +5-V housekeeping supply.

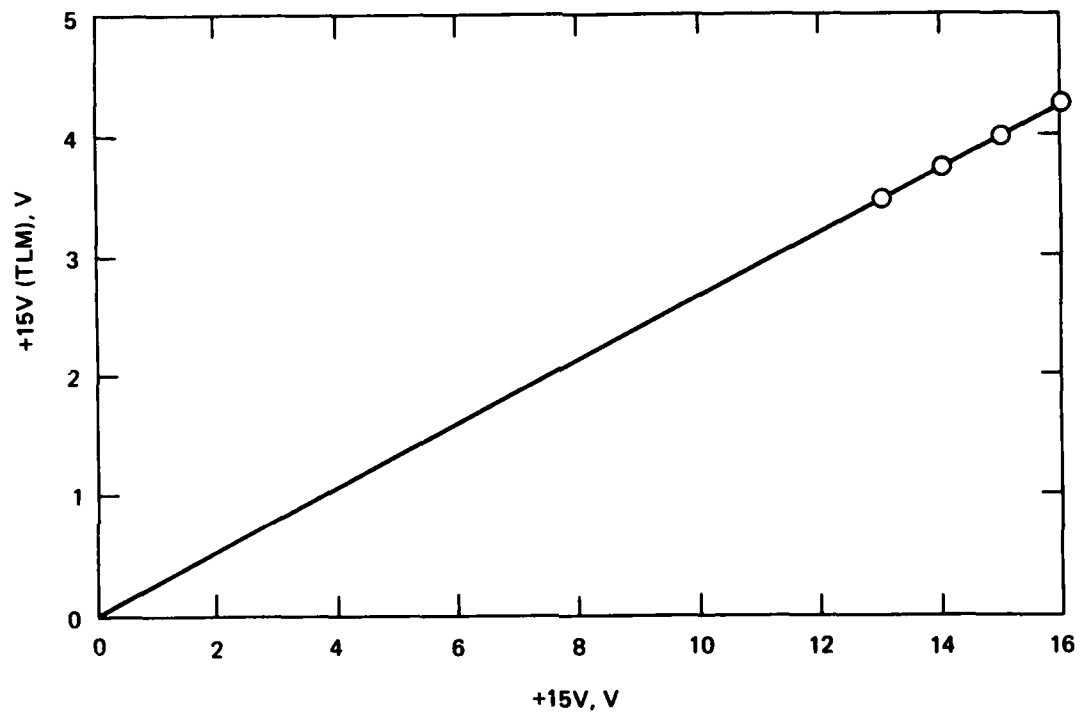


Figure 6-20. Telemetry calibration curve for the +15-V housekeeping supply.

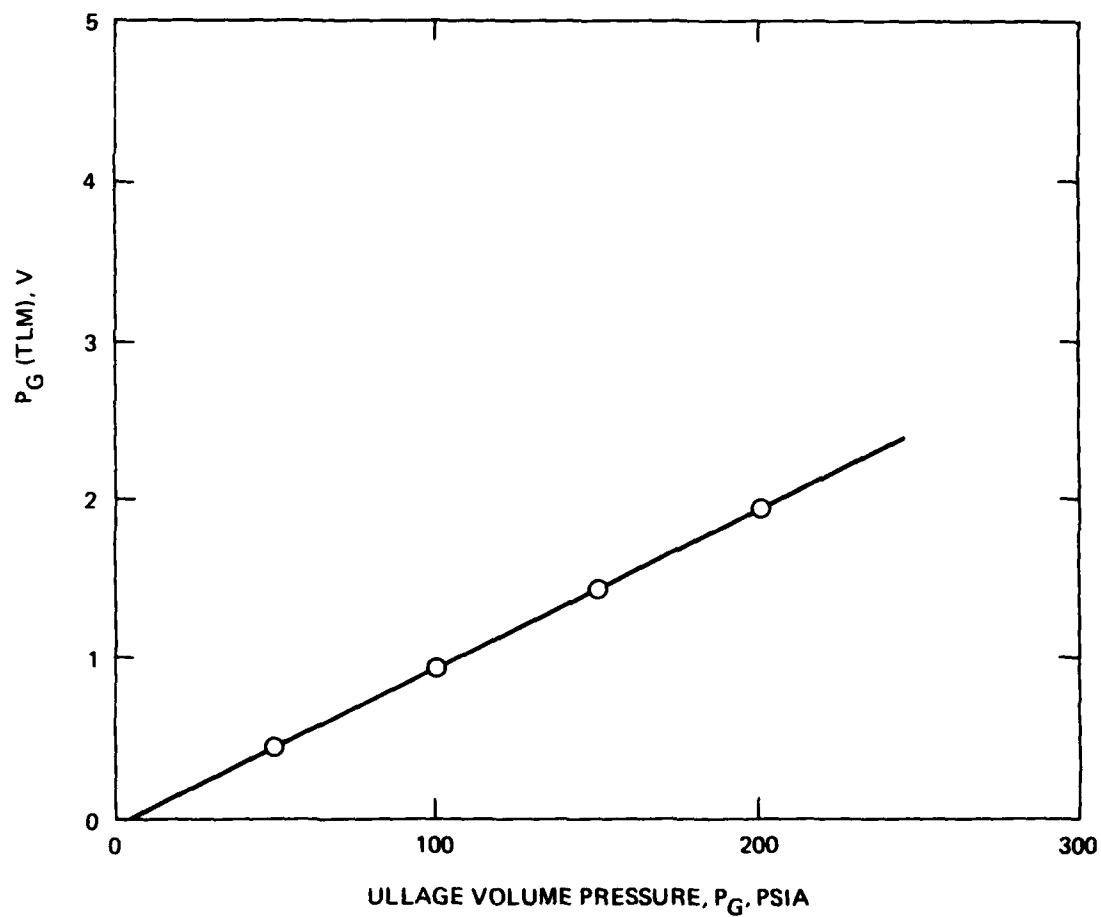


Figure 6-21. Telemetry calibration curve for the ullage volume pressure.

SECTION 7

GROUND SUPPORT EQUIPMENT (GSE)

The ground support equipment (GSE) is microprocessor controlled with a disk-based operating system. It employs the S-100 bus and contains mainly Cromemco hardware. A photograph of the GSE is shown in Figure 7-1.

Manual commands can be entered by depressing one key to set any of the current and voltage setpoints, turn the source ON and OFF, and OPEN and CLOSE the gas valve. A ramp command is available to automatically ramp through the current and voltage setpoints. The starting and ending current, starting and ending energy, and dwell time per step for the ramp command can also be easily set. The telemetry parameters are converted from analog to digital and displayed on a video screen in engineering units, along with the command stored in the command latch of the PEU. The date and time are also displayed. The software and hardware of the GSE will drive a parallel-input type printer which can be commanded to print manually or automatically in time increments of one minute (1, 2, 3. ... minutes). A typical printout is shown in Figure 7-2 where

VF is the filament voltage in V,
IF is the filament current in A,
VD is the discharge voltage in V,
ID is the discharge current in A,
VA is the accel voltage in V,
IA is the accel current in A,
VS is the screen voltage in V,
IS is the screen current in A,
I3 is the decel current in A,

IE is the emission current in A,
PT is the power to the source in W,
V15 is the 15 V housekeeping bus in V,
V5 is the 5 V housekeeping bus in V,
PG is the ullage volume pressure in kPa, and
STAT is the command word stored in the command
latch (in hexadecimal).

15479-47

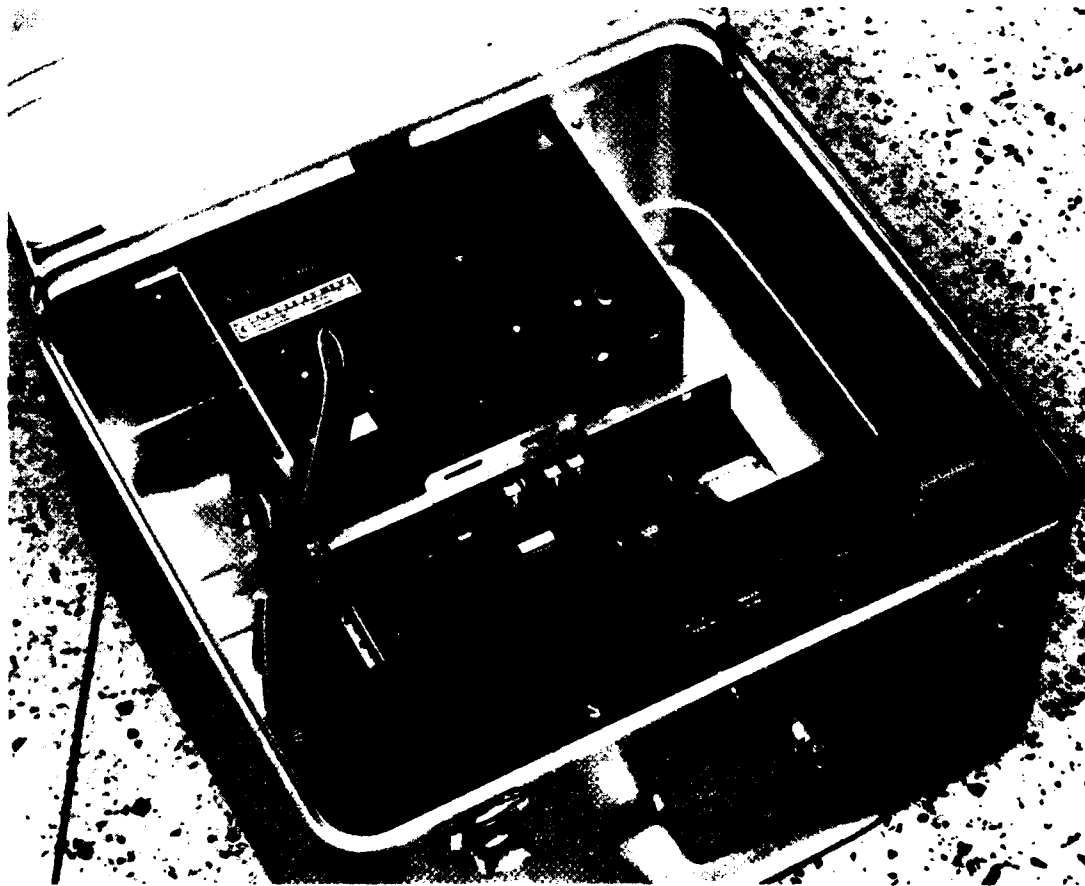


Figure 7-1. Photograph of the ground support equipment.

07:36:20 PM	TUE 07/17/84			
VF= 5.0869	VD= 136.08	VA= 521.226	VS= 4658.4	STAT=4B
IF= 4.80249	ID= 0.008854	IA= 0	IS= 0.0001597	I3= 3.764E-05
IE= 9.03947E-05	PT= 26.3786	V15= 15.6555	V5= 5.292	PG= 0
07:36:30 PM	TUE 07/17/84			
VF= 5.16516	VD= 136.08	VA= 523.744	VS= 4658.4	STAT=5B
IF= 4.87509	ID= 0.013281	IA= 0	IS= 0.0003194	I3= 3.764E-05
IE= 1.51493E-04	PT= 28.4758	V15= 15.6555	V5= 5.292	PG= 0
07:36:50 PM	TUE 07/17/84			
VF= 5.24342	VD= 136.08	VA= 523.744	VS= 4658.4	STAT=6B
IF= 4.91139	ID= 0.013281	IA= 0	IS= 0.0004791	I3= 3.764E-05
IE= 2.44002E-04	PT= 29.7916	V15= 15.6555	V5= 5.292	PG= 0
07:37:00 PM	TUE 07/17/84			
VF= 5.24342	VD= 136.08	VA= 521.226	VS= 4658.4	STAT=7B
IF= 4.91139	ID= 0.017708	IA= 0	IS= 0.0006388	I3= 5.646E-05
IE= 0.000393	PT= 31.138	V15= 15.6555	VS= 5.292	PG= 0
07:37:10 PM	TUE 07/17/84			
VF= 5.32168	VD= 135	VA= 523.744	VS= 4658.4	STAT=8B
IF= 4.94769	ID= 0.022135	IA= 0	IS= 0.0009582	I3= 7.528E-05
IE= 6.58632E-04	PT= 33.7819	V15= 15.6555	V5= 5.292	PG= 0
07:37:30 PM	TUE 07/17/84			
VF= 5.32168	VD= 135	VA= 521.226	VS= 4638.99	STAT=9B
IF= 4.98399	ID= 0.026562	IA= 0	IS= 0.0014373	I3= 0.0000941
IE= 1.10381E-03	PT= 36.7767	V15= 15.6555	V5= 5.292	PG= 0
07:37:40 PM	TUE 07/17/84			
VF= 5.39994	VD= 125.28	VA= 523.744	VS= 4638.99	STAT=AB
IF= 5.02029	ID= 0.030989	IA= 0	IS= 0.0020761	I3= 1.1292E-04
IE= 1.77784E-03	PT= 40.6226	V15= 15.6555	V5= 5.292	PG= 0

Figure 7-2. A typical printout from the GSE.

END
FILMED

5-86

DTIC